Deep–Sea Research II 199 (2022) 105079

Contents lists available at ScienceDirect

Deep-Sea Research Part II

journal homepage: www.elsevier.com/locate/dsr2

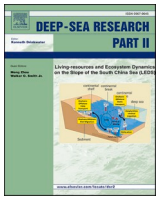

Spatial and temporal variability of Net Primary Production on the Agulhas Bank, 1998–2018

Sixolile L. Mazwane [a,*], Alex J. Poulton [b], Anna E. Hickman [c], Fatma Jebri [d], Zoe Jacobs [d], Mike Roberts [a,d], Margaux Noyon [a]

[a] Department of Oceanography and Institute for Coastal and Marine Research, Nelson Mandela University, Gqeberha, 6001, South Africa
[b] The Lyell Centre for Earth and Marine Science and Technology, Heriot-Watt University, Riccarton Campus, Edinburgh, EH14 4AP, UK
[c] University of Southampton, National Oceanography Centre Southampton, European Way, Southampton, SO14 3ZH, UK
[d] National Oceanography Centre, Southampton, SO14 3ZH, United Kingdom

ARTICLE INFO

Keywords:
Net primary production
Remote sensing
Phytoplankton
Continental shelf
Upwelling
Vertically generalized production model

ABSTRACT

Despite the importance of Agulhas Bank (AB) marine productivity in supporting South African coastal fisheries and shelf ecosystems, there are relatively few regional-scale assessments of its spatial and temporal variability, and most productivity studies have been limited in scale. Here we use satellite-derived Net Primary Production (NPP) rates calculated using the Vertically Generalized Production Model (VGPM) to examine the spatial and temporal dynamics of NPP over the 21-year satellite record (1998–2018) on the AB. In calculating VGPM NPP we used the OCCI Chlorophyll-*a* product, SST from Operational-Sea-Surface-Temperature-and-Sea-Ice-Analysis (OSTIA) and PAR from GlobColour level-3 mapped products as these represent the longest datasets that fit our extended study period. We examine spatial trends between the eastern and central AB, as well as three areas of the bank (around Port Alfred, the Tsitsikamma coast, and the 'cold ridge') that have been previously identified as contributing significantly to the overall productivity of the AB. The AB shows only a moderate degree of seasonality in NPP calculated from the VGPM, with NPP being highest in austral summer (1.7–1.8 g C m^{-2} d^{-1}) and lowest in winter (0.9–1.0 g C m^{-2} d^{-1}), and remains relatively high (>1 g C m^{-2} d^{-1}) throughout the year, contrasting sharply with other shelf systems. Considered annually, NPP on the bank was 516 g C m^{-2} yr^{-1} (38 Mt C yr^{-1} when scaled to the total shelf area) which is higher than many other shelf systems though lower than the neighbouring Benguela system and is indicative of a moderately productive shelf system fuelled by perennial NPP. Comparing different sections of the AB from east to central bank, and including the three upwelling areas, highlighted that spatial differences in NPP were relatively limited; that these three upwelling areas made similar contributions to their relative proportion of the total shelf area, and that average rates of NPP are spatially similar across the bank, though notable high rates occur in some coastal upwelling areas. Interannual variability in NPP was relatively modest, varying between years by only ~15% over the two decades assessed. Over the 21-year data set, there was a slight (~0.26% yr^{-1}) statistically-significant decline in calculated NPP over time for the AB as a whole, which, when examined on a pixel-by-pixel basis, indicated that most of the decline was on the central bank between 100 m and 200 m isobaths. In summer, an increase in NPP occurred on the EAB (26.5–28°E). In conclusion, the AB is a significant site of perennial moderate levels of NPP, varying little interannually and with only a slight decline in NPP over time. These factors lead to a stable environment in terms of ecosystem productivity so that the AB makes a significant contribution to the productivity of South African regional fisheries.

1. Introduction

Continental shelf seas are important areas that play a major role in global ocean primary production (Simpson and Sharples, 2012), representing ~10% of the global ocean and ~15–30% of global primary production (Bauer et al., 2013; Lohrenz et al., 2002; Muller-Karger et al., 2005). Shelf seas generate biological production that supports over 90% of global fish catches (Pauly et al., 2002), and therefore represent key

* Corresponding author.
E-mail address: Smazwane46@gmail.com (S.L. Mazwane).

https://doi.org/10.1016/j.dsr2.2022.105079
Received 1 February 2021; Received in revised form 4 March 2022; Accepted 27 March 2022
Available online 8 April 2022

systems in supporting economic activities (Watson and Pauly, 2001). Primary production is crucial to sustaining marine food webs, from zooplankton to higher trophic levels, such as fish and marine mammals. Coastal and shelf seas are also important net sinks of atmospheric carbon dioxide (globally 0.4 Pg C yr^{-1}; e.g., Thomas et al., 2004). The Agulhas Bank (AB) is considered one of the most productive shelf seas in the Southern Indian Ocean, with high chlorophyll-*a* concentrations (>2 mg m^{-3}), and is of significant economic importance to South Africa, supporting major spawning grounds for commercially important species including anchovy, sardine, squid, hake, kingklip, sole and yellowtail (Hutchings, 1994; Hutchings et al., 2002). After spawning on the AB, some fish larvae and juveniles are transported toward the southwestern African coast where they grow within the nutrient-rich and productive waters of the Benguela upwelling system (Hutchings et al., 2002).

The AB is described as a 'triangular shape' that ranges from Cape Point (18 °E) in the west to East London, 800 km to the east (Probyn et al., 1994) (Fig. 1). On the western side of the AB, the Benguela current flows in a northward direction. On the eastern side of the AB, parallel to the 200 m isobath, flows the Agulhas Current (AC), one of the strongest western boundary currents in the world (Lutjeharms, 2006a) which transports large amounts of warm (>18 °C), salty and nutrient-poor surface waters southwards from the Indian Ocean. The AC retroflects southwest of the AB, creating an off-shelf area of intense eddy activity composed of meanders, eddies and filaments (Gordon, 2003).

Due to current-driven upwelling along the continental slope, sometimes termed 'Ekman veering' (Chapman and Largier, 1989), deep, relatively cold nutrient-rich waters are advected up the slope and onto the shelf, leading to strong on-shelf transport along the whole east and central AB. On the narrow eastern AB (EAB), this leads to a strong thermocline with temperature differences of 8–10 °C, frequently termed a "double layer system" (e.g., Swart and Largier, 1987). The influence of the AC is often more pronounced on the EAB, potentially reaching as far on-shelf as the coast (Lutjeharms, 2006b) rather than further west where the shelf is broader (Fig. 1; Jury, 1994). In summer, stratification is intensified by increasing solar radiation and an increase in the speed of the AC, leading to more advection of cold bottom waters onto the bank (Hutchinson et al., 2018). The surface layer of the AB results from the mixing of Sub-Tropical Indian Waters and AC waters (McMurray, 1989), while the bottom water originates from intermediate South Indian Ocean Central Water with cool temperatures (<12 °C) and is relatively nutrient-rich (Lutjeharms, 2006a). Further to the west, stratification is enhanced by cyclonic frontal eddies which force further warm Sub-Tropical Indian Waters and cold South Indian Ocean Central Water onto the shelf (Swart and Largier, 1987). The winter situation has been much less studied and only Eppley et al. (1985) have described a well-mixed water column in winter, but the degree to which there is winter overturning of the water column on the AB is unclear. Swart and Largier (1987) suggested that stratification breaks down in winter over much of the AB, apart from on the EAB and the outer shelf where it is sustained the whole year round due to Ekman veering and interaction with the AC.

While the outer shelf is influenced by oceanic forces, the inner bank is affected by coastal wind-driven processes (Boyd and Shillington, 1994). Due to the orientation of the coast, winds with an easterly component, which are more prevalent in summer, favour the upwelling of cold nutrient-rich waters near Port Alfred and in the capes of Algoa Bay and St Francis Bay, as well as along the Tsitsikamma coast, while westerly winds are more common in winter (Boyd and Shillington, 1994). Over most of the outer AB, the flow is in a south-westward direction and is parallel to the isobath of the bank (Boyd et al., 1992). This general flow is interrupted by mesoscale, short-lived structures, such as cyclonic eddies and meanders, which can induce counter-currents on the AB (Lutjeharms, 2006a). On the inner shelf of the central AB (CAB), several studies have shown that the current is mostly eastwards, especially along the Tsitsikamma coast (Boyd et al., 1992; Hutchings, 1994; Roberts and van den Berg, 2005). These differences in currents between the outer and inner shelf may also produce areas of recirculation and water retention (Schumann, 1987; Boyd and Shillington, 1994).

Phytoplankton growth and primary production are primarily controlled by the availability of nutrients and irradiance (e.g., Beardall et al., 2001; McQuatters-gollop et al., 2011), while mortality factors such as zooplankton grazing and viral lysis are important loss processes. Areas of enhanced primary productivity, such as continental shelves, are often the product of increased nutrient inputs from oceanic deep water, as well as riverine input. In the case of the AB, riverine nutrient sources are likely to be minimal due to low rainfall over the continent (SAWS, 2020), so nutrient supply to the AB is mainly through the upwelling of South Indian Ocean Central Water onto the shelf and nutrient cycling and retention in the bottom water layers.

Net Primary Production (NPP) represents total (or gross) primary

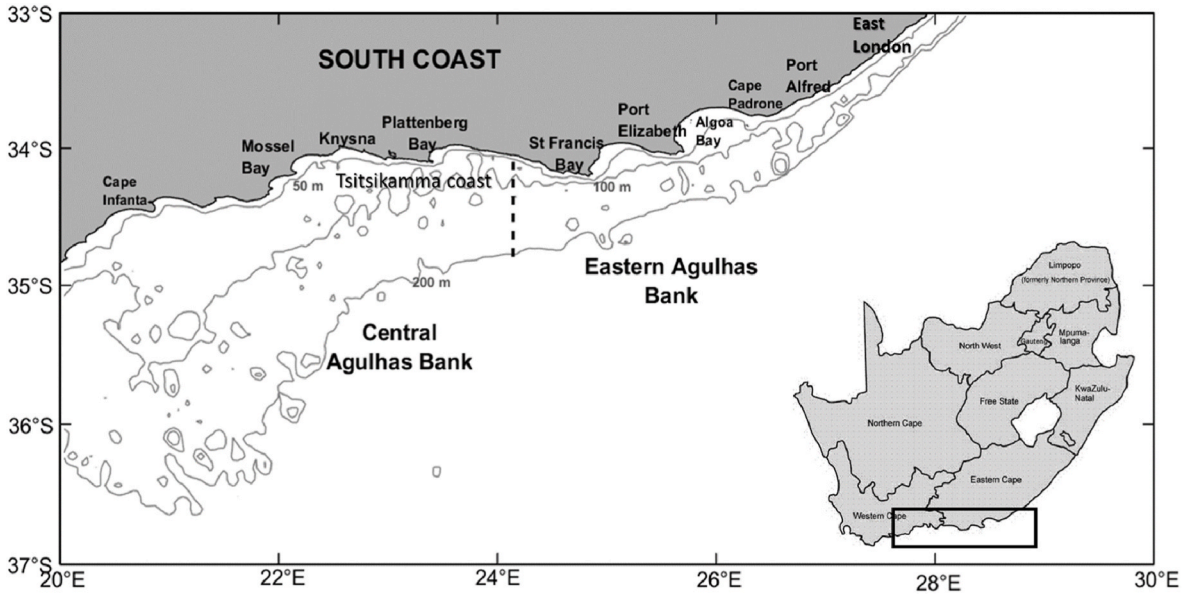

Fig. 1. Map of the Central and Eastern Agulhas Bank, South Africa and its bathymetry (grey lines). The vertical dashed black line at 24°E shows the separation used in this study to separate the eastern and central Agulhas Bank. The Southernmost boundary of the bank domain considered is the 200m isobath.

production minus the losses due to phytoplankton respiration and the release of dissolved organic carbon (Behrenfeld et al., 2006; Muller-Karger et al., 2005). NPP is the primary source of organic matter for export to higher trophic levels. Due to the sparsity of *in-situ* measurements of NPP in the ocean, it is difficult to fully resolve spatial and temporal variability using field measurements alone. Primary production can be determined in various ways, using different methodologies or combinations of data, including satellite chlorophyll-*a*, sea surface temperature (SST), Photosynthetically Active Radiation (PAR) and *in-situ* chlorophyll-*a* (e.g., Balkanski et al., 1999; Smyth et al., 2004; Lee et al., 2015; Ma et al., 2014). There are several satellite products available for surface chlorophyll-*a* concentrations which vary in terms of length of the record and are often blended products from multiple satellite-based sensors. Individually, ocean colour sensors have different lifespans and sensitivities, causing inherent bias and occasionally making comparisons difficult (Racault et al., 2017), leading to the need for blending of multiple products to obtain a long-term dataset. The OC-CCI chlorophyll-*a* product that was used in this study (OC-CCIv4.2), for instance, blends five single sensors to allow for a 21-year (1997–2012) global scale, climate-quality controlled, bias-corrected, and error characterised data record of ocean colour (Sathyendranath et al., 2020).

In this study we applied the Vertically Generalized Production Model (VGPM) of Behrenfeld and Falkowski (1997). The VGPM is considered to provide reasonable estimates of NPP at both global and regional scales (e.g., Behrenfeld and Falkowski, 1997; Kahru et al., 2009; Muller-Karger et al., 2005; Yamada et al., 2005) when compared to other satellite-based NPP models (Kahru et al., 2009; Cervantes-Duarte et al., 2021). For example, a comparative study of various NPP models (i.e., the Eppley Square Root (ESQRT) (Eppley et al., 1985), the VGPM, the Kameda and Ishizaka (2005) (KI) model, the Marra et al. (2003) model (MARRA), the Carbon-based Production Model (CbPM) (Behrenfeld et al., 2005), and a version of the VGPM after linear regression (VGPM-CAL) (Kahru et al., 2009) revealed that the VGPM was the most accurate model when compared to *in-situ* data (Kahru et al., 2009; Deng et al., 2017). It has also been used successfully to assess NPP in several other shelf seas (e.g., Lomas et al., 2012; Cervantes-Duarte et al., 2021).

In addition to allowing reasonable estimates of NPP for regional-scale studies, the VGPM has the advantage of being a relatively simple model to apply, and all the parameters used in the model can be directly or indirectly derived from remotely-sensed data (Mizobata and Saitoh, 2004; Kameda and Ishizaka, 2005; Yamada et al., 2005; Li et al., 2020). However, the VGPM does have recognized limitations, mainly being that it ignores photo-acclimation and simply equates chlorophyll-*a* concentration to phytoplankton standing (carbon) biomass (Taboada et al., 2019). Another recognized limitation is that it estimates the maximum rates of productivity through a simple relationship with SST rather than factoring in the effects of nutrients or variable community composition (Behrenfeld and Falkowski, 1997).

To date, very few studies have used satellite-derived data to determine the magnitude and/or variability of NPP on the AB (e.g., Demarcq et al., 2008). Previous *in-situ* measurements of NPP on the AB are scarce and only available from relatively short-term (<1 month) research cruises. Of the limited number of coastal studies on the CAB and EAB, most were made in the late 1980s and 1990s (Brown, 1984; McMurray, 1989; Hutchings, 1994; Probyn et al., 1994), with a few recent studies in the early 2000s (Barlow et al., 2010). In summer, *in-situ* studies indicate that the western AB usually has lower subsurface chlorophyll-*a* concentrations (0.5–6 mg m^{-3}) compared to the EAB (1–15 mg m^{-3}) (McMurray, 1989). Daily *in-situ* measurements of NPP on the AB vary from 0.27 to 9.6 g C m^{-2} d^{-1} (Brown, 1984; Hutchings, 1994; Probyn et al., 1994; Barlow et al., 2009, 2010; Boyd et al., 2014) which is in the range of other shelf seas (e.g., Benguela, Barlow et al., 2009; North western European Shelf, Poulton et al., 2014; Celtic Sea, Poulton et al., 2019), though these measurements are all spatially and temporally biased.

In-situ NPP observations on the AB indicate strong spatial and temporal variability, ranging from 0.3 to 1.1 g C m^{-2} d^{-1} associated with localized areas of high productivity, such as the 'cold ridge', Port Alfred upwelling cell (Lutjeharms, 2006a) and the Tsitsikamma coast (Duncan et al., 2019). Also, amongst the few shelf-wide studies that have measured NPP across the EAB and CAB (e.g., Barlow et al., 2010), there has been a bias towards spring and summer periods (Probyn et al., 1995). A synoptic view of the AB is currently lacking though there has been a previous satellite-based assessment of NPP which was included in a wider assessment and comparison of the western, southern and eastern shelf systems of South Africa (Demarcq et al., 2008). The study by Demarcq et al. (2008), based on satellite data from September 1997 to August 2003 and using a broad-band light transmission model for estimating NPP, found that NPP ranged from 0.7 to 2.4 g C m^{-2} d^{-1} on the AB. Demarcq et al. (2008) concluded that the AB exhibited little seasonal variability and was less productive (0.75–1.5 g C m^{-2} d^{-1}) than the Benguela upwelling system on the west South African coast, but more productive (1–2 g C m^{-2} d^{-1}) than the eastern shelf (20–25°E).

As the AB supports considerable socio-economically important fisheries and marine ecosystems, understanding the spatial and temporal (seasonal, interannual) variability of NPP is a high priority. Gaining a synoptic overview of NPP on the AB, contrasting the dynamics of the shelf with other shelf systems, and comparing a regional view with patchy *in-situ* NPP measurements from the literature, are all key objectives to assess NPP on the AB and elucidate how it supports a productive marine ecosystem. With this in mind, we set out to address the following specific research questions: (1) What is the magnitude and spatial distribution of NPP on the AB? (2) What is the magnitude of interannual and seasonal variability of NPP on the AB? (3) How does a synoptic satellite view of NPP on the AB compare with the previous spatially and temporally biased *in-situ* measurements? and (4) How do the dynamics of NPP on the AB compare with other shelf systems at a similar latitude? Using freely available satellite data from 1998 to 2018, we directly address these key research questions for the AB.

2. Material and methods

2.1. Primary production model

The Vertically Generalized Production Model (VGPM) proposed by Behrenfeld and Falkowski (1997) was used in this study. The algorithm requires several variables that can be obtained from *in-situ* and satellite observations.

$$PP_{eu} = 0.66125 \times P^{B}_{opt} \times \frac{E_0}{E_0 + 4.1} \times Z_{eu} \times C_{opt} \times D_{irr} \quad (1)$$

where *PPeu* is the euphotic zone integrated primary production (mg C m^{-2} d^{-1}), P^{B}_{opt} is the maximum primary production per unit of chlorophyll-*a* in the vertical profile (mg C (mg Chl-a^{-1}) hr^{-1}), E_0 is the daily PAR (E m^{-2} d^{-1}) at the sea surface, Z_{eu} is the depth of the euphotic zone (m) calculated using K_d490 (i.e. $K_{avg} = \ln(0.01)/Z_{eu}$), C_{opt} is the sea surface chlorophyll-*a* concentration (mg m^{-3}), and D_{irr} is day length (hrs). P^{B}_{opt} is expressed by Behrenfeld and Falkowski (1997) as a 7th order polynomial of temperature (T) as follows:

$$P^{B}opt = -3.27 \times 10^{-8}T^{7} + 3.4132 \times 10^{-6}T^{6} - 1.348 \times 10^{-4}T^{5} + 2.462 \times 10^{-3}T^{4} - 0.0205T^{3} + 0.0617T^{2} + 0.2749T + 1.2956 \quad (2)$$

The accuracy of the VGPM model has been tested by comparing the algorithm estimates to ^{14}C based NPP estimates and other satellite-based productivity algorithms (Campbell et al., 2002), and it has been used to study global primary production over both relatively short intra-annual (e.g., Behrenfeld et al., 2001) and decadal scales (e.g., Gregg et al., 2003), as well as being widely used for ocean primary production estimates (e.g., Behrenfeld and Falkowski, 1997; Deng et al., 2017).

2.2. Satellite data

The satellite-derived variables considered in this study are chlorophyll-*a*, downwelling light attenuation coefficient at 490 nm (K_d490), used to calculate the depth of the euphotic zone in equation (1), Photosynthetically Active Radiation (PAR), and Sea Surface Temperature (SST) fields. The chlorophyll-*a* and K_d490 datasets were obtained from the Ocean-Colour Climate Change Initiative project (OC–CCI version 4.2; http://www.esaoceancolour-cci.org/) at a spatial resolution of 4 km and on a monthly basis from January 1998 to December 2018.

The OC-CCI chlorophyll-*a* product (OC-CCIv4.2; 1997-present) is a blended product built by merging measurements from the Sea-viewing Wide Field-of-View Sensor (SeaWIFS, 1997–2010), Medium Resolution Imaging Spectrometer (MERIS, 2002 to 2012), Moderate Resolution Imaging Spectroradiometer (MODIS, 2002-present), Visible Infrared Imaging Radiometer Suite (VIIRS, 2012-present), and the Sentinel-3 Ocean and Land Color Instrument (OLCI-3A, 2016-present). The OC-CCI chlorophyll-*a* data are the most consistent timeseries of multi-satellite global ocean colour data currently available (Racault et al., 2017; Sathyendranath et al., 2020). This chlorophyll-*a* product provides more than 21 years of observations which is considered of the highest quality and suitable for analysis of long-term variability (Sathyendranath et al., 2020; Kulk et al., 2021). The OC-CCI product is considered especially reliable given that this is a longer merged dataset than single sensor timeseries and additionally features corrected drift in the MODIS sensor (Jackson et al., 2020). The multi-sensor OC-CCI product also features MERIS which gets closer to the coasts than the other ocean colour sensors and provides, overall, an improved performance in Case-2 (coastal) waters, as well as Case-1 open waters (Jackson et al., 2020).

Chlorophyll-*a* observations may be overestimated in shallow optically complex Case II waters, where suspended sediments and/or coloured dissolved organic matter do not covary in a predictable manner with chlorophyll-*a* (IOCCG, 2000). As the majority of the AB comprises Case-I open waters (Morel et al., 2006; Zhang et al., 2006; Demarcq et al., 2008), this issue likely affects only a small proportion of the data (i.e., the areas shallower than ~30 m and thus representing a very narrow coastal band; see bathymetry on Fig. 1). The CCI K_d490 data is derived using the Lee et al. (2005) equation and backscattering coefficient of pure water (bbw) from Zhang and Hu (2009), following the SeaDAS Kd_Lee algorithm. The algorithm was designed for optically deep waters, and thus is generally limited in its applicability for measurements contaminated by bottom reflectance (Barnes et al., 2013), such as shallow (<30 m) coastal waters.

Photosynthetically Active Radiation (PAR) (E m^{-2} d^{-1}) data was obtained from GlobColour level-3 mapped products (http://hermes.acri.fr/index.php?class=archive) and represents the mean daily photon flux density in the visible range (400–700 nm) that can be used for photosynthesis (Hooker et al., 2003). As per the other two datasets, the monthly PAR data from January 1998 to December 2018 is used in this study.

The SST data used in this study is the reprocessed L4 product acquired from the Operational-Sea-Surface-Temperature-and-Sea-Ice-Analysis (OSTIA). This is a multi-satellite global dataset that is freely downloadable from the Copernicus Marine Environment Monitoring Service (CMEMS) (http://marine.copernicus.eu/services-portfolio/access-to-products/). The SST data are provided daily at a spatial resolution of 5 km, and from 1985 to 2018. Although this SST product spans the period 1985 to 2018, only the period 1998 to 2018 was used here to be consistent with the remotely sensed chlorophyll-*a* and K_d490 datasets. We computed monthly means over the AB region during the study period of 1998–2018.

To examine the winds on the AB, we used the ERA-5 reanalysis of 10 m zonal and meridional winds produced by the European Centre for Medium-Range Weather Forecasts (ECMWF). This dataset was obtained from the Climate Data Store (CDS) dataset (https://cds.climate.copernicus.eu/cdsapp#!/dataset/reanalysis-era5-single-levels-monthlymeans? tab = overview; Hersbach et al., 2020) at a horizontal spatial resolution of 25 km as monthly averages from 1979 to present. We considered the period 1998 to 2018 to calculate the climatological means of wind fields to match the NPP data. We included the average wind speed, as well as the meridional (v; E to W) and zonal (u; N to S) components. Wind speed was calculated as the square root of the sum of u squared and v squared components (Grange, 2014), and all three variables were averaged identically as the NPP.

2.3. Spatial analysis

The AB in this study is delimited to the south by the 200 m isobath and excludes the western AB, which is part of the Benguela upwelling system. This work forms part of a larger project (SOLSTICE-WIO; Roberts, *this issue*), in which a consistent delimitation between the EAB and CAB was selected at 24 °E (see also Chang, 2008) to ensure consistency between studies. In the literature, hotspots of enhanced chlorophyll-*a* biomass, linked to upwelling areas on the AB, have been identified and we investigated these in detail in this study. Based on previous studies (Carter et al., 1987; Swart and Largier, 1987; Probyn et al., 1994; Malan, 2013) highlighting several high chlorophyll-*a* regions on the AB, we selected three regional boxes to examine in detail: Port Alfred on the EAB, the Tsitsikamma coast and the cold ridge area on the CAB (Fig. 2a).

3. Results

3.1. Net Primary Production on the Agulhas Bank

Over the 21-year period of satellite data, monthly average daily NPP (g C m^{-2} d^{-1}) on the AB ranged from 0.12 to 11.08 g C m^{-2} d^{-1}, with an overall timeseries average (± standard deviation) of 1.04 (±0.29) g C m^{-2} d^{-1}. The average daily NPP was statistically higher on the EAB than on the CAB (Table 1; $p < 0.001$, Wilcoxon rank sum test). Comparison between the three upwelling sites showed timeseries average daily NPP in the Port Alfred region (see Fig. 2) of 1.69 (±0.15) g C m^{-2} d^{-1}, with 1.59 (±0.13) g C m^{-2} d^{-1} on the Tsitsikamma coast and 1.38 (±0.09) g C m^{-2} d^{-1} in the cold ridge area (Table 1). These rates of average daily NPP are statistically different from each other ($p < 0.001$, Wilcoxon rank sum tests), indicating dissimilar levels of daily NPP between these three regions of interest.

Monthly averages of daily NPP were scaled to annual NPP (g C m^{-2} yr^{-1}) for the 21-year study period for the entire AB (Fig. 2) and each specified region of the bank (Table 1). Across the 21-year study period, the annual NPP on the AB ranged from 300 to 770 g C m^{-2} yr^{-1}, with a timeseries average annual NPP of 516 (±77) g C m^{-2} yr^{-1}. High average annual NPP was observed along the coast on both the CAB and EAB (>600 g C m^{-2} yr^{-1}) (Fig. 2a). The EAB showed significantly higher annual NPP (596 ± 45 g C m^{-2} yr^{-1}) compared with the CAB (493 ± 68 g C m^{-2} yr^{-1}) (Table 1, see also Fig. 2a, $p < 0.001$, Wilcoxon rank sum test). There was elevated NPP (relative to the open ocean) off the AB, along the shelf edge, although the values were lower (average of waters deeper than 200 m: 331 g C m^{-2} yr^{-1}) than the average estimated for the AB (<200m). The coefficient of variation of annual NPP shows ~1–5% variability on the EAB and 5–12% on the CAB (Fig. 2b). Port Alfred and the Tsitsikamma coast showed a higher range of annual NPP (488–656 g C m^{-2} yr^{-1}) compared to the cold ridge (~400–570 g C m^{-2} yr^{-1}) (Table 1; $p < 0.001$, Wilcoxon rank sum tests; see Fig. 2a).

3.2. Seasonal variability of Net Primary Production on the Agulhas Bank

The AB climatology of NPP over the 21-year time series reveals that monthly averages of daily NPP ranged from 0.9 to 1.8 g C m^{-2} d^{-1} (Fig. 3), with an annual average of 1.04 (±0.3) g C m^{-2} d^{-1} (Table 1) for the AB. The absolute variability of average monthly NPP for the AB is ~1 g C m^{-2} d^{-1} (range: 0.8–1 g C m^{-2} d^{-1}); (Fig. 3). The seasonal pattern in the three upwelling cells followed the same general seasonal

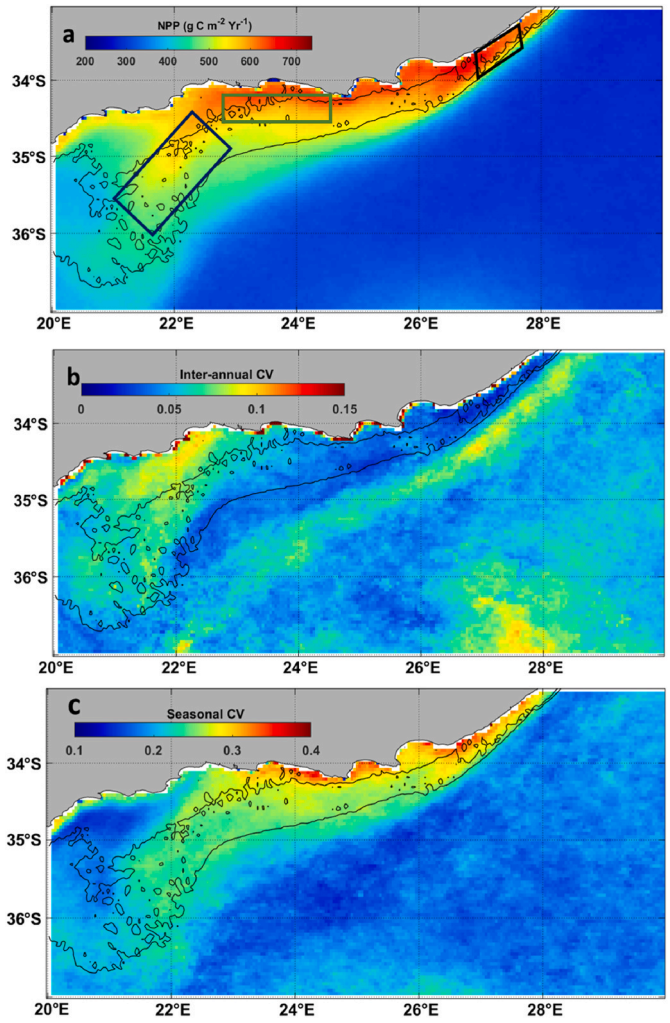

Fig. 2. Distribution of (a) monthly-average annual Net Primary Production (g C m^{-2} yr^{-1}), (b) variability in terms of the coefficient of variation on the Agulhas Bank (1998 – 2018), and (c) seasonal variability in terms of the coefficient of variation on the Agulhas Bank. The average annual NPP (a) over the whole shelf is 516 g C m^{-2} yr^{-1}, with variability (b) taken as the standard deviation of the annual NPP for each year divided by the mean of the annual values over the whole time series for each pixel. Grey and black lines indicate the 100 m (inner shelf) and 200 m (outer shelf) bathymetric lines, respectively. The different coloured boxes in (a) represent the selected upwelling cells on the bank for this study: black is Port Alfred, green is the Tsitsikamma coast, and blue is the cold ridge. White pixels close to the coastline indicate no data.

trend as for the whole AB, with peak values in January of ~2.2 g C m^{-2} d^{-1} on the Tsitsikamma coast and ~2.4 g C m^{-2} d^{-1} in Port Alfred in December, while the cold ridge was relatively lower at ~1.8 g C m^{-2} d^{-1} (Fig. 3). Overall, the NPP values on the cold ridge across the whole year were more similar in magnitude to the whole AB, whereas Port Alfred and the Tsitsikamma coast were consistently higher by 0.1–0.2 g C m^{-2} d^{-1}, and even more so during the summer upwelling season (up to ~0.6 g C m^{-2} d^{-1}, Fig. 3).

In summer, relatively high NPP (>2 g C m^{-2} d^{-1}) occurs across much of the Agulhas Bank (Fig. 4). The NPP distribution in autumn is relatively similar in distribution to the summer but at a lower general level of NPP (1.2–1.5 g m^{-2} d^{-1}). During both summer and autumn, relatively high NPP is constrained to the eastern side of the AB with slightly higher NPP around the cold ridge area compared with the rest of the bank. In contrast to the other months, winter has low levels of NPP throughout the AB (Fig. 4). Spring NPP is relatively similar throughout the AB (~1.5 g C m^{-2} d^{-1}), similar to summer and autumn, although of an

Table 1
Satellite Net Primary Production (NPP) estimates (1998–2018) using the VGPM Model (Behrenfeld and Falkowski, 1997) for the Agulhas Bank (AB), separated into CAB and EAB, and the specific upwelling regions (cold ridge, Tsitsikamma Coast, Port Alfred). Included in the table is the area of each region (km^2), the timeseries-average daily NPP (g C m^{-2} d^{-1} ± SD) and annual NPP (g C m^{-2} yr^{-1} ± SD), and the areal average annual NPP per region (Mt C yr^{-1} ± SD). Values in brackets give the percentage contribution for each region to the total area of the Agulhas Bank and total areal NPP.

Region	Region area, km^2 (%)	Daily NPP, g C m^{-2} d^{-1}	Average Annual NPP, g C m^{-2} yr^{-1}	Areal annual NPP, Mt C yr^{-1} (%)
Agulhas Bank (AB)	75, 120 (100)	1.04 ± 0.29	516 ± 77	38.0 ± 1.4 (100)
Central Agulhas Bank (CAB)	57, 856 (77)	1.37 ± 0.19	493 ± 68	28.1 ± 1.3 (75)
Eastern Agulhas Bank (EAB)	17, 264 (23)	1.67 ± 0.11	596 ± 45	9.8 ± 0.3 (25)
Cold Ridge	10, 928 (15)	1.38 ± 0.09	497 ± 36	5.4 ± 0.3 (14)
Tsitsikamma Coast	10, 864 (14)	1.59 ± 0.13	570 ± 50	6.9 ± 0.2 (16)
Port Alfred	3, 296 (4)	1.69 ± 0.15	608 ± 53	2.0 ± 0.04 (5)

intermediate magnitude between the other two seasons (Fig. 4). Comparing the average percentage contributions (± standard deviations) for each season in terms of annual NPP (Table 2), summer NPP contributes 30.2 ± 1.5% (range: 28–31%), with autumn contributing 26.8 ± 1.0% (26–28%) and spring and winter NPP representing lower contributions to annual NPP of 20.0 ± 1.3% (19–22%) and 23.0 ± 1.1% (22–24%), respectively. These contributions of seasonal NPP to annual NPP highlight that there are almost equal contributions for the different seasons (i.e., close to 25% for each season). Examining how this seasonal variability was spatially distributed, the seasonal coefficient of variation showed 25%–40% variation, with a distinct increasing gradient along the coast from east to west (Fig. 2c). The NPP on the central CAB along the cold ridge area showed 25% variability between seasons and low variability (10%–20%) was observed further west on the central CAB, between ~21 °E and 22°E.

3.3. Interannual variability of NPP on the Agulhas Bank

To examine temporal variability in NPP across the AB from 1998 to 2018, we plotted a Hovmöller diagram that shows a clear longitudinal pattern in NPP throughout the 21 years (Fig. 5), with higher NPP from approximately 22 °E to 27.5 °E compared to the western side of the CAB. The east-west pattern is even more apparent during the productive summer months (December–February). Across the 21-year dataset there was noticeable variability, with a geographic restriction of the productive waters in some years (i.e., restricted to the EAB; see e.g., 2006 and 2017, Fig. 5 and Supplementary Fig. S1) or reduced NPP in the winter and spring months (e.g., 2012 and 2013). The year 2009 was particularly interesting as it had one of the highest daily NPP in summer, combined with the lowest winter daily NPP recorded over the 21-year period (Fig. 5; see also Fig. S1). Several years had high NPP on the EAB all the way west of 22 °E, sometimes even extending to 20 °E (e.g., end 2008), reaching values up to ~ 2.8 g C m^{-2} d^{-1}. In this case, several of these years also seemed to have experienced a more productive spring period compared to others (e.g., 2011 and 2016), while other years had extremely intense summer periods of NPP (e.g., 1999, 2009 and 2010; Fig. 5; see also Fig. S1).

To further examine how such interannual variability in the spatial extent and magnitude of NPP influenced the annual productivity on the AB, we scaled the annual NPP on the AB to the entire shelf. Between 1998 and 2018, annual NPP for the whole AB ranged from 35 to 40 Mt C yr^{-1}, with an average of 38.0 (±1.1) Mt C yr^{-1} (Table 1; Fig. 6a). When

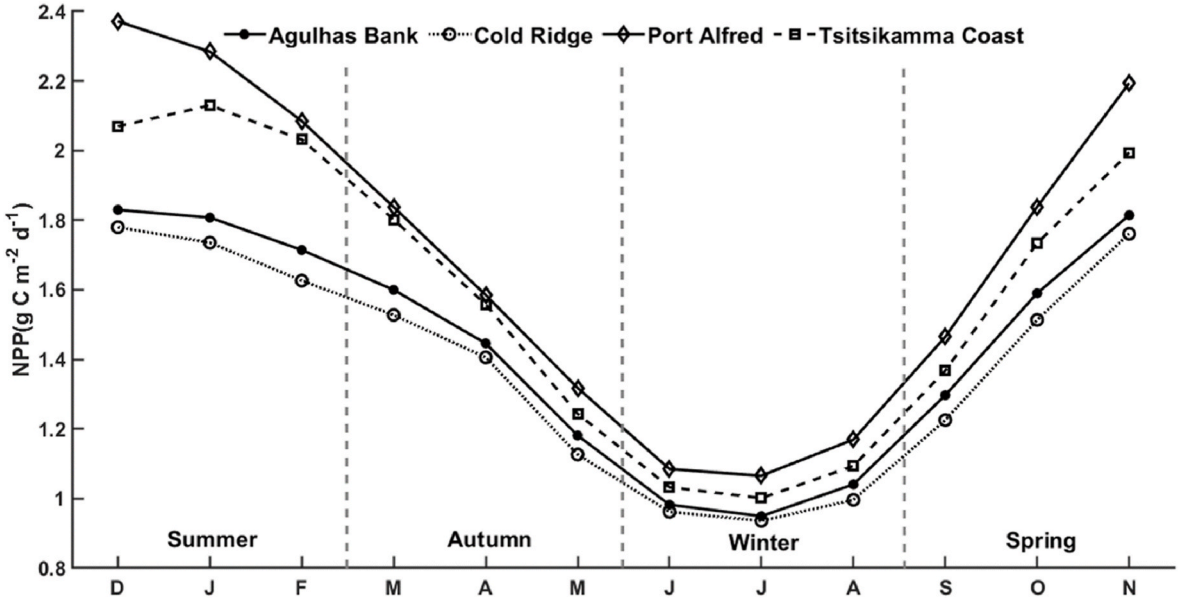

Fig. 3. Monthly average-derived daily NPP (g C m^{-2} d^{-1}) for the AB and the different upwelling regions of the Agulhas Bank examined in this study, averaged from 1998-2018. Seasonal extents are indicated with vertical dashed lines.

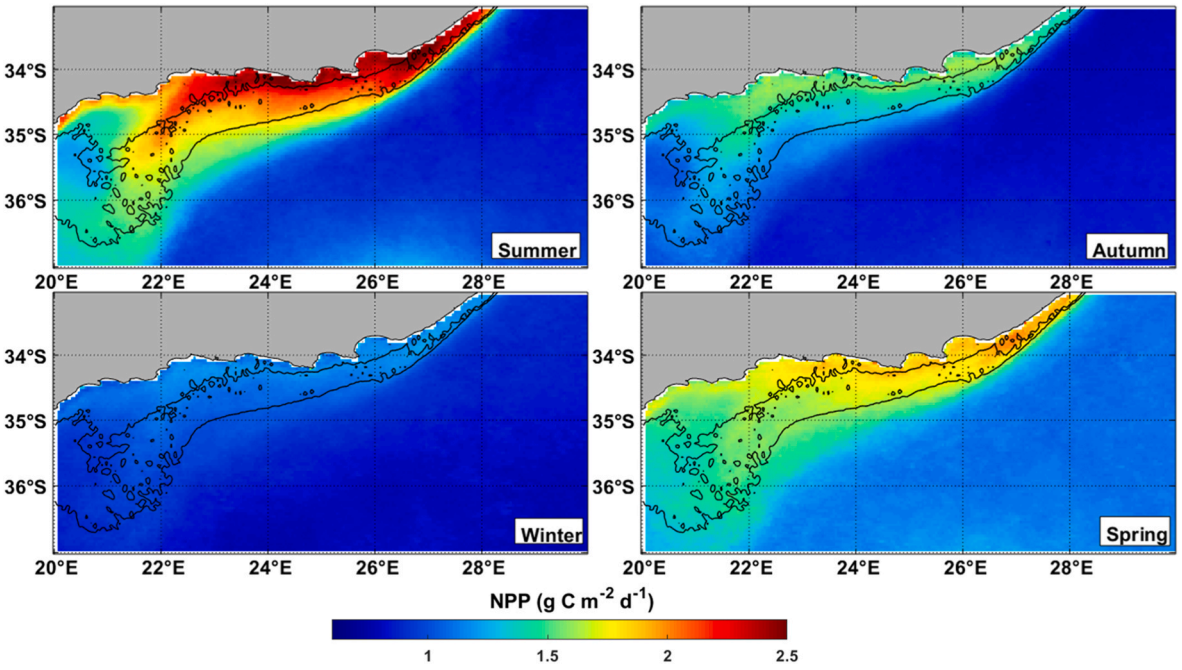

Fig. 4. Seasonal maps showing spatial pattern of NPP (g C m-2 d-1) on the AB for the 21-year study period (1998 – 2018).

plotted for each year over the 21-year dataset, annual NPP exhibited a statistically significant decrease (linear regression: $y = -0.103x + 244.27$, $R^2 = 0.18$, $p = 0.05$), declining by ~ 0.26% (~0.10 Mt C) each year (Fig. 6a) or ~5.5% over the entire time series. Delineating the whole AB into different regions showed, unsurprisingly, that the larger CAB had higher annual NPP (28.1 ± 1.31 Mt C yr^{-1}; ~75% of total AB productivity) compared to the smaller EAB (9.8 ± 0.25 Mt C yr^{-1}; ~25% of total), following the proportion of the surface area of each section of the bank (23% and 77%, respectively, Table 1). In terms of the three regions of interest, the smaller Port Alfred region had the lowest annual NPP (2.0 ± 0.04 Mt C yr^{-1}; 5% of total NPP), while the cold ridge and Tsitsikamma coast had higher and similar levels of NPP (5.4 ± 0.28 and 6.9 ± 0.24 Mt C yr^{-1}, respectively; 14% and 16%, respectively (Table 1; Fig. 6b).

Examining the full 21-year dataset, of the regions examined only the EAB, Tsitsikamma coast and cold ridge had statistically significant long-term changes (declines) in NPP ($y = -0.0185x + 46.92$; $R^2 = 0.21$; $p < 0.05$ and $y = -0.0209x + 48.31$; $R^2 = 0.29$; $p < 0.01$ and $y = -0.0019x + 43.96$; $R^2 = 0.18$; $p = 0.05$, respectively), while the CAB and Port Alfred region showed no statistically significant trend over time (Fig. 6a and b). In terms of magnitude, the decline on the EAB was of the order of 0.05% yr^{-1} (~0.02 Mt C yr^{-1}) and on the Tsitsikamma Coast the trend was ~0.06% yr^{-1} (~0.02 Mt C yr^{-1}). To gain further spatial insights into these trends of NPP, a pixel-by-pixel analysis was also performed. For each pixel, a linear regression was fitted on the 21 years of NPP values (g C m^{-2} d^{-1}), with only the significant slopes shown (p-value > 0.05)

Table 2
Annual Net Primary Production (g C m^{-2} yr^{-1} ± SD) and seasonal percentage contributions for different regions and upwelling sites on the bank.

Region	Annual NPP (g C m^{-2} yr^{-1})	Seasonal contributions (%)			
		Summer (DJF)	Autumn (MAM)	Winter (JJA)	Spring (SON)
Agulhas Bank	516 ± 77	31	26	19	24
Central Agulhas Bank (CAB)	493 ± 68	32	26	19	24
Eastern Agulhas Bank (EAB)	596 ± 45	29	28	21	22
Cold Ridge (CR)	497 ± 36	31	26	19	24
Tsitsikamma Coast	570 ± 50	30	27	20	22
Port Alfred	608 ± 53	28	28	22	22

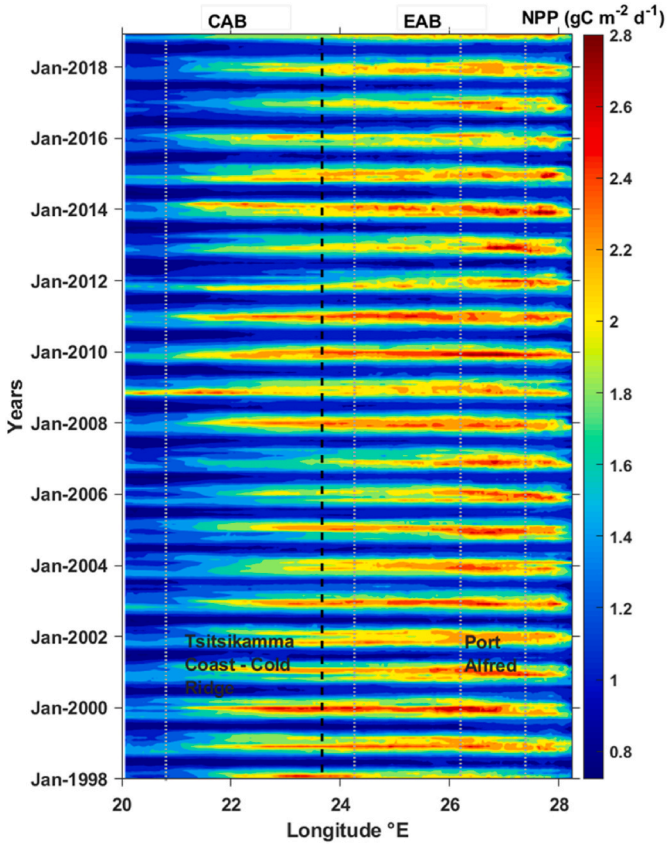

Fig. 5. Hovmöller diagram of NPP (g C m^{-2} d^{-1}) over the AB shelf (0 –200 m) from 20°S to 28.25°S for the period January 1998 to December 2018.

(Fig. 6c). Examining these long-term trends in NPP on a pixel-by-pixel basis showed a declining trend in the deeper waters (>100 m) of the CAB between 22°E and 24 °E, also west of 21°E, whereas no significant trends were detected for the rest of the AB. In summer, on the EAB (26.5°E to 28°E) there was an increase in NPP over time and a decline between 100 m and 200m isobath from 22°E to 26.5°E. In winter and spring, there was a decline in the NPP over time, mostly limited between 100 m and 200 m isobaths (Fig. S2).

4. Discussion

4.1. Net Primary Production on the Agulhas Bank

This is the first study based on satellite derived NPP using the VGPM to examine long-term (21 years) spatial and temporal trends of NPP on the central and eastern AB. *In-situ* NPP measurements on the CAB and EAB, using ^{13}C and ^{14}C methods, are relatively rare (see Table 2), with far more NPP studies focusing on the western coast of South Africa (i.e., the Benguela upwelling). Of the limited number of coastal studies on the CAB and EAB, most were made in the late 1980s and 1990s (Brown, 1984; McMurray, 1989; Hutchings, 1994; Probyn et al., 1994) though several more recent studies have occurred in the last decade (Barlow et al., 2010; Poulton et al., *this issue*). Our monthly average-derived daily estimates of NPP satellite-derived (based on VGPM) for the AB (0.9–1.8 g C m^{-2} d^{-1}) fall well within the range of NPP measurements from *in-situ* studies (Table 2). For example, NPP of 0.3–3.6 g C m^{-2} d^{-1} were found on the southeast coast, 0.3–3.7 g C m^{-2} d^{-1} for the Natal Bight (Barlow et al., 2010), and 0.1–1.1 g C m^{-2} d^{-1} for the AB in autumn (Poulton et al., *this issue*) (see Table 3). Compared to the neighbouring Benguela ecosystem, our satellite-derived NPP estimates from the AB were lower than *in-situ* measurements in summer (2.4 g C m^{-2} d^{-1}) but more similar or slightly higher than in winter (0.9 g C m^{-2} d^{-1}) (Barlow et al., 2010).

Considering satellite-derived NPP, Demarcq et al. (2008) used a broad-band light transmission model to derive NPP for the three shelf systems of South Africa and their values (0.6–2.5 g C m^{-2} d^{-1}) agree well with our VGPM-derived values (Fig. 3). Further, Demarcq et al. (2008) found that the seasonal variability of the AB had a lower magnitude (0.9–1.4 g C m^{-2} d^{-1}) than the other sectors of the South African coastline, such as the Benguela upwelling (1.2–2.1 g C m^{-2} d^{-1}). The climatology of NPP on the AB over the 21 years shows a range in NPP from 0.9 to 1.8 g C m^{-2} d^{-1} (Fig. 3), with the highest values found during summer (Fig. 3). When compared with other shelf systems, from various latitudes, where the NPP has also been derived from remote sensing, we see comparable levels of NPP. For example, Curran et al. (2018) examined the Northwestern European shelf and found NPP estimates ranging from 0.2 to 0.9 g C m^{-2} d^{-1} from winter to autumn, while a similar study by Joint et al. (2001) found annual NPP ranging from 0.2 to 1.4 g C m^{-2} d^{-1}. On the Northwest Iberian Margin, Beca--Carretero et al. (2019) estimated NPP to range from 0.4 to 1.4 g C m^{-2} d^{-1}, throughout the year. In contrast, satellite studies on the Chilean shelf by Testa et al. (2018) observed lower winter NPP (0.2–0.8 g C m^{-2} d^{-1}) and higher summer NPP (1.8–6.4 g C m^{-2} d^{-1}) compared to the AB. Similarly, in Southeast Australia, monthly NPP showed low winter NPP (<2.0 g C m^{-2} d^{-1}) and high summer NPP (~8.0 g C m^{-2} d^{-1}) (Thompson and Mcdonald, 2020). While the AB does not experience the extremely high NPP observed in other locations (e.g., Chilean Shelf, Southeast Australia, Benguela), it does have similar NPP to many other shelf systems (e.g., Northwestern European Shelf, Northwest Iberian Margin), although there is a limit to the number of comparisons possible due to only a small number of shelf systems being studied by remote sensing.

Annual NPP for the AB in this study was 516 g C m^{-2} yr^{-1} (Fig. 2, Table 1), with a range of 300–677 g C m^{-2} yr^{-1} across the AB (Fig. 2a). In general, the annual NPP for the AB is higher than those determined for the global coastal zone by Longhurst et al. (1995) of 385 g C m^{-2} yr^{-1} or by Boyd et al. (2014) of 250–300 g C m^{-2} yr^{-1}, implying that NPP in the shelf waters of the AB is 1.3–2 times higher than many other coastal areas. Demarcq et al. (2008) estimated an annual average NPP for the AB that was also higher than many coastal areas (438 g C m^{-2} yr^{-1}), though lower than our estimates. In contrast, using limited *in-situ* measurements, Probyn et al. (1994) estimated annual estimates for the whole AB of 656 g C m^{-2} yr^{-1} from 1981 to 1992 (~30 measurements), which are more similar in magnitude to our estimates, although at the high end. Compared to the southern Benguela system, Lamont (2011) found surprisingly higher annual mean NPP estimates (799 and 1032 g C m^{-2} yr^{-1}, based on satellite data) than on the AB. For example, in Bahia de La Paz (Mexico, 24–25 °N), the annual average NPP were more similar to global averages at 350 g C m^{-2} yr^{-1} (Verdugo-Díaz et al., 2014) and 432 g C m^{-2} yr^{-1} (Cervantes-Duarte et al., 2021). In summary, the AB is as productive as many other shelf seas, with winter NPP relatively high compared to the summer NPP (i.e., weak seasonal difference). However,

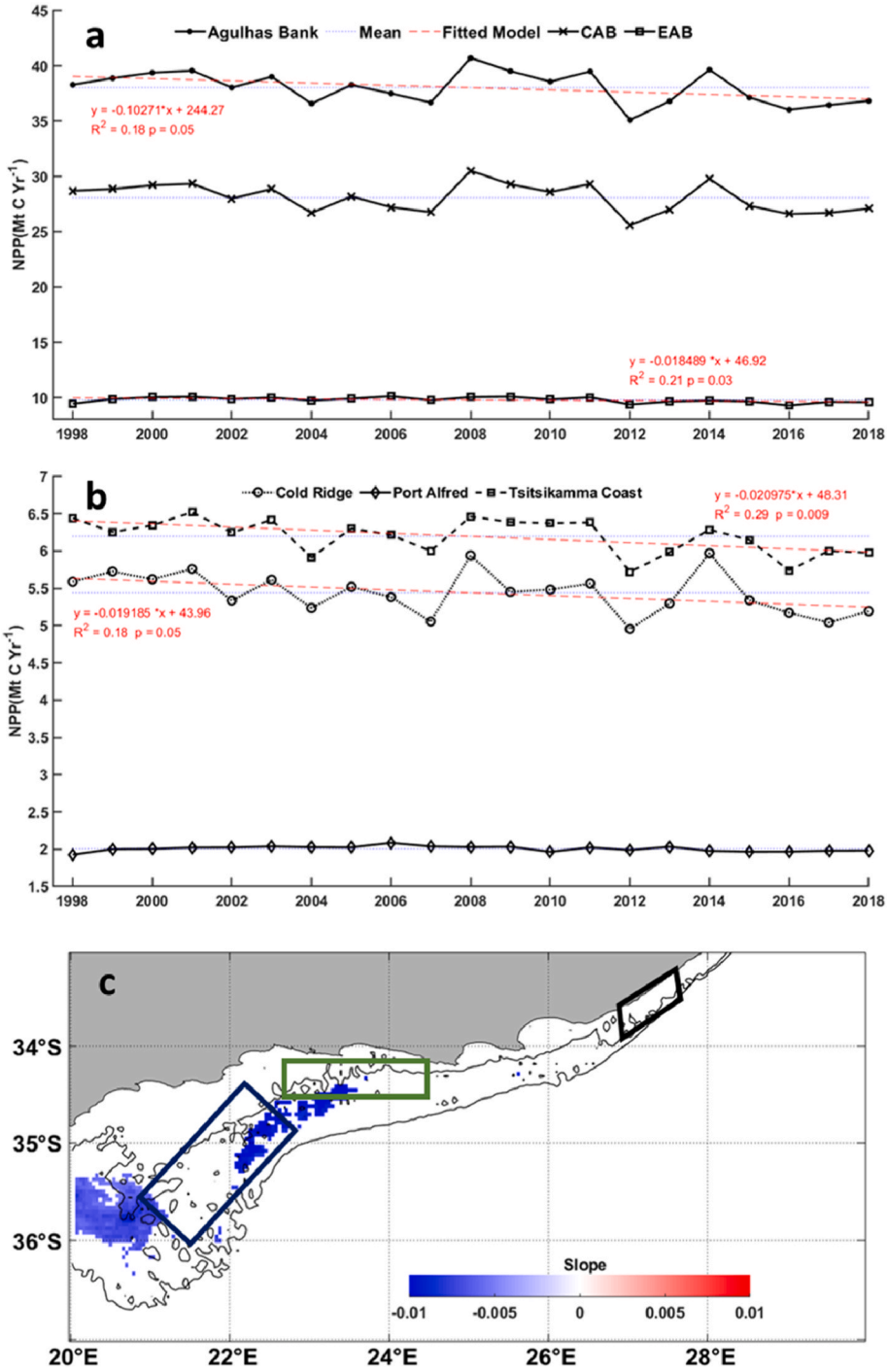

Fig. 6. Annual Net Primary Production (NPP; Mt C yr^{-1}) on the Agulhas Bank (AB) between 1998 and 2018 derived from the Vertically Generalized Production Model (VGPM, Behrenfeld and Falkowski, 1997), (a) NPP of the whole AB (AB), central AB (CAB) and eastern AB (EAB) and (b) upwelling regions on the AB. Horizontal dashed grey line indicates the 21-year average (38.03 ± 1.5 Mt C yr^{-1}) for the Agulhas Bank, and the red dashed lines are fitted linear regressions for: (a) AB (y = -0.1027x + 244.2; R^2 = 0.18; p = 0.05) showing a 0.10 Mt decline over the timeseries, CAB (y = -0.084x + 197.3; R^2 = 0.16; p = 0.07) and EAB (y = -0.0184x + 46.92; R^2 = 0.21; p < 0.05); (b) Tsitsikamma coast (y = -0.0209x + 48.31; R^2 = 0.29; p < 0.01); cold ridge (y = -0.0192x + 43.96, R2 = 0.18, p = 0.05) and Port Alfred (y = -0.0014x + 4.74, R2 = 0.05, p > 0.05), and (c) Pixel-by-pixel examination of the trend in NPP over the 21 years showing statistically significant (p < 0.05) slopes of the fitted linear regression. The red colour shows a negative slope and the red colour shows a positive slope.

on a global scale, it only represents 0.3% of coastal NPP (based on an estimate of global NPP for the coastal province of 14 Gt C yr^{-1}; Longhurst et al., 1995).

4.2. *Spatial variability of Net Primary Production on the Agulhas Bank*

We observed an east-to-west trend of declining production (Fig. 5; see also Fig. S1), with higher NPP on the eastern part of the AB throughout the year (average of 1.67 g C m^{-2} d^{-1} in the EAB relative to 1.37 g C m^{-2} d^{-1} in the CAB). This confirms previous spatially limited surveys that have observed a strong east-to-west gradient in NPP (e.g., Hutchings, 1994; Probyn et al., 1994, Demarcq et al., 2008; Poulton et al., *this issue*). The same pattern was also observed by Demarcq et al. (2008) where these authors estimated an average NPP close to 1.5 g C m^{-2} d^{-1} on the eastern bank (including the central bank), while Poulton et al. (*this issue*) observed patchy NPP across the entire AB, although the CAB had lower NPP in general.

Flowing along the shelf edge of the AB is the warm oligotrophic Agulhas Current, which has a strong influence on the oceanography of the AB (e.g., Jackson et al., 2012; Goschen et al., 2015). Generally, NPP was higher on the AB (<200 m) than off-shelf in the Agulhas Current (>200 m isobath) (Fig. 2). There was slightly elevated NPP observed along the shelf edge and beyond the 200 m isobath, but these levels of NPP were still lower than that of waters shallower than 200 m (Fig. 2). This was also observed by Demarcq et al. (2008) on both the eastern and central AB, where they estimated values less than 1 g C m^{-2} d^{-1} in the

Table 3
Estimates of NPP (g C m^{-2} d^{-1}) along the South African coast.

Region	Season	Daily NPP (g C m^{-2} d^{-1})	Method	Reference
Agulhas Bank	Summer	1.8	VGPM	This study
	Autumn	1.4		
	Winter	1.0		
	Spring	1.6		
Agulhas Bank	Autumn	0.3–1.1	*In-situ*	Poulton et al., *this issue*
		0.1–1.1	Chl-*a*	
Agulhas Bank	Summer	2.0	*In-situ*	Probyn et al. (1994)
Agulhas Bank	Summer	1.4	Integrated Chl-*a* and light model	Demarcq et al. (2008)
	Autumn	1.0		
	Winter	0.9		
	Spring	1.4		
Eastern Agulhas Bank	Summer	4.8–9.6		Hutchings (1994)
Eastern Agulhas Bank	Spring	0.5–0.8	*In-situ*	Brown (1984)
South east coast of SA	Spring	0.3–3.6	*In-situ*	Barlow et al. (2010)
Natal Bight	Spring	0.3–3.7	*In-situ*	Barlow et al. (2010)
Benguela Ecosystem	Summer	2.4	*In-situ*	Barlow et al. (2009)
	Winter	0.9		

Agulhas Current and higher values on the AB (up to 3 g C m^{-2} d^{-1}). Nutrients to support NPP can either be brought up to the surface by coastal upwelling or from external sources such as river input. In comparison to the nutrient-rich underlying South Indian Ocean Water, the surface water of the Agulhas Current is considered to be nutrient-poor, so that when it encroaches onto the shelf, it brings very little nutrients but warms the surface waters (Lutjeharms et al., 1996). Rather, the Agulhas Current induces current-driven upwelling of this nutrient-rich South Indian Central Water into the bottom layer of the South African continental shelf, thereby increasing the nutrient concentrations available to be upwelled into the surface waters and thus stimulating primary production (Lutjeharms, 2006b).

The higher productivity on the EAB is linked to the topography of the shelf and the presence of the Agulhas Current. The EAB, compared to further west, is narrow and thus the nutrient-enriched waters pushed onto the shelf along the shelf break, due to the current-driven upwelling (i.e., Ekman veering), are spread over the whole width of the narrow bank, all the way to the coast (Hutchings, 1994; Lutjeharms, 2006a, 2006b; Goschen et al., 2015). This nutrient-enriched water is then brought to the surface due to wind-driven upwelling during easterlies, or the thermocline may be shallow enough to penetrate the euphotic layer and thus enhance primary production (Goschen et al., 2012; Duncan et al., 2019). The divergence of isobaths away from the coast as the shelf widens southwards of Port Alfred also contributes to this upwelling (Gill and Schumann, 1979). The Tsitsikamma coast also presented high NPP and is known as a region of coastal upwelling induced by easterly winds (Roberts and van den Berg, 2005; Goschen and Schumann, 2011; Duncan et al., 2019).

The line of a continuous coastal maximum of NPP observed on the AB (Fig. 2) may be the result of coastal wind-driven upwelling along the coast near Port Alfred, Cape padrone (Goschen et al., 2015) and Tsitsikamma (Duncan et al., 2019). A similar coastal maximum of chlorophyll-*a* was observed by Probyn et al. (1994) from *in-situ* measurements. This continuous coastal maximum is mostly visible in summer and autumn, and coincides with easterly winds that occur in summer, resulting in wind-driven upwelling along the Tsitsikamma coast and Port Alfred area.

On the CAB, along the 100 m isobath, high NPP was observed in some years in the area identified previously as the 'cold ridge' (CR, Fig. S1). Boyd and Shillington (1994) suggested that where the bank widens, the flow on the inner shelf, influenced by wind-driven forcing and the Agulhas Current flowing on the outer shelf, creates a divergence contributing to the upwelling of a tongue of cold water enriched in nutrients in the area of the CR. Later, based on remote sensing observations of surface temperatures, this phenomenon (CR) was hypothesized to be coupled with the coastal wind-driven upwelling off the Tsitsikamma coast and was referred to as a 'filament' (Walker, 1986; Roberts, 2005) though it was noted that the CR does not occur for each coastal upwelling event. Lutjeharms (2006a) suggested that cold water was being upwelled on the EAB and then transported on the shelf towards the west. A 1/4° resolution ROMS model revealed that without any Agulhas Current, the CR disappears from simulations, and concluded that the CR was most likely under an oceanic influence (Chang, 2008). Using a 1/12° high-resolution ocean model, Jacobs et al. (*this issue*) found that the highest productivity on the CAB occurs when there are strong easterly winds, initiating upwelling on the EAB, and fast currents on the AB which advect nutrient-rich water westward, initiating phytoplankton blooms in the vicinity of the CR.

Whether the mechanisms involved are linked to localized enriched upwelled water or just due to the circulation pattern on the shelf, this study shows that, over most of the year, the region along the 100 m isobath of the CAB has high NPP (Fig. 2a) which agrees with previous observations (Carter et al., 1987; Probyn et al., 1994; Swart and Largier, 1987). This also coincides with a high-resolution ocean model with average values ranging from 0.8 to 1.3 g C m^{-2} d^{-1} (Jacobs et al., *this issue*). It is worth noting that a tongue of cold water, that is the CR, has, however, not been observed in seasonal sea surface temperature (Fig. S4). This highlights that the CR is not necessarily linked to the upwelling of cold water, or that the phenomenon does not reach the surface, or that monthly averages (in NPP) are not adequate to show upwelling that lasts only a few days. If this region of enhanced NPP was visible on annual estimates using monthly averages, it would indicate that this region has enhanced NPP most of the time.

Finally, it is interesting to note that on the inner bank, where the shelf is at its widest (i.e., west of Mossel Bay and shallower than 100 m), annual NPP is low (<500 g C m^{-2} yr^{-1}, see Fig. S1). This region has been hypothesized to be a region of re-circulation, with eastward currents (Boyd and Shillington, 1994; Goschen and Schumann, 1994). If low NPP often occurs in this zone, on the inshore side of the CR, this might also contribute to the shape of the so-called CR as a tongue of NPP surrounded by the Agulhas Current on one side and a cyclonic recirculation cell on the inside, both low in NPP.

One of our objectives was to test whether previously identified NPP hotspots contributed significantly to the overall NPP of the bank, as implied in much of the literature. Comparison of the areal (cumulative) annual NPP for the different sections of the AB highlights that differences between zones are due to both significantly higher NPP rates and also differences in the areal extent of each zone (Table 1). The sparse *in-situ* NPP estimates observed in the past give a partly biased image of the NPP on the AB as they have mainly concentrated on the upwelling areas as the main sites of NPP for the AB. The satellite observations of NPP shown here highlight that the upwelling sites, despite having higher NPP rates, make up a minor fraction of the total NPP on the whole AB and have a limited impact on the whole shelf NPP. In effect, the satellite data shows that the AB as a whole is a productive environment, not just the specific upwelling sites (e.g., Port Alfred upwelling) highlighted in the literature (e.g., Probyn et al., 1994; Malan, 2013). This finding reframes our understanding of NPP and ecosystem productivity of the AB, shifting the focus from specific regional sites to a more holistic shelf-wide view of enhanced production in support of marine food webs and socio-economically important fisheries.

4.3. Seasonal variability of Net Primary Production on the Agulhas Bank

The monthly climatology of NPP on the AB showed a clear seasonal cycle with higher NPP in summer (1.9 g C m^{-2} d^{-1}), and lower NPP in

winter (0.9 g C m^{-2} d^{-1}). Demarcq et al. (2008) observed a similar pattern to this, with the lowest NPP occurring in winter (0.9 g C m^{-2} d^{-1}) and the highest occurring in summer (1.4 g C m^{-2} d^{-1}). The parameters driving the NPP estimated using the VGPM, are chlorophyll-*a*, light and SST which all show a clear seasonal cycle (Fig. 7). Overall chlorophyll-*a* was higher (~0.8–1 mg m^{-3}) in autumn and spring than in summer and winter for the AB (Fig. 7a). In terms of the specific zones of the AB, this trend in chlorophyll-*a* was similar for the cold ridge area, but with lower concentrations, while Tsitsikamma showed more difference between the minimums and maximums (~0.6 mg m^{-3}). This pattern was quite different for the Port Alfred region with the highest values (~1.4 mg m^{-3}) from November to December (late spring/early summer), ~1.5 mg m^{-3} in March (autumn), and the lowest values from July to August (~0.8 mg m^{-3}) (Fig. 7a). High light levels (PAR) were observed in summer and spring, with decreasing light levels (as low as 20 E m^{-2} d^{-1}) in autumn and winter, with no difference between the AB and any of the three specific upwelling zones (Fig. 7b). Warmer surface waters were observed in summer (>20 °C) and spring, with colder

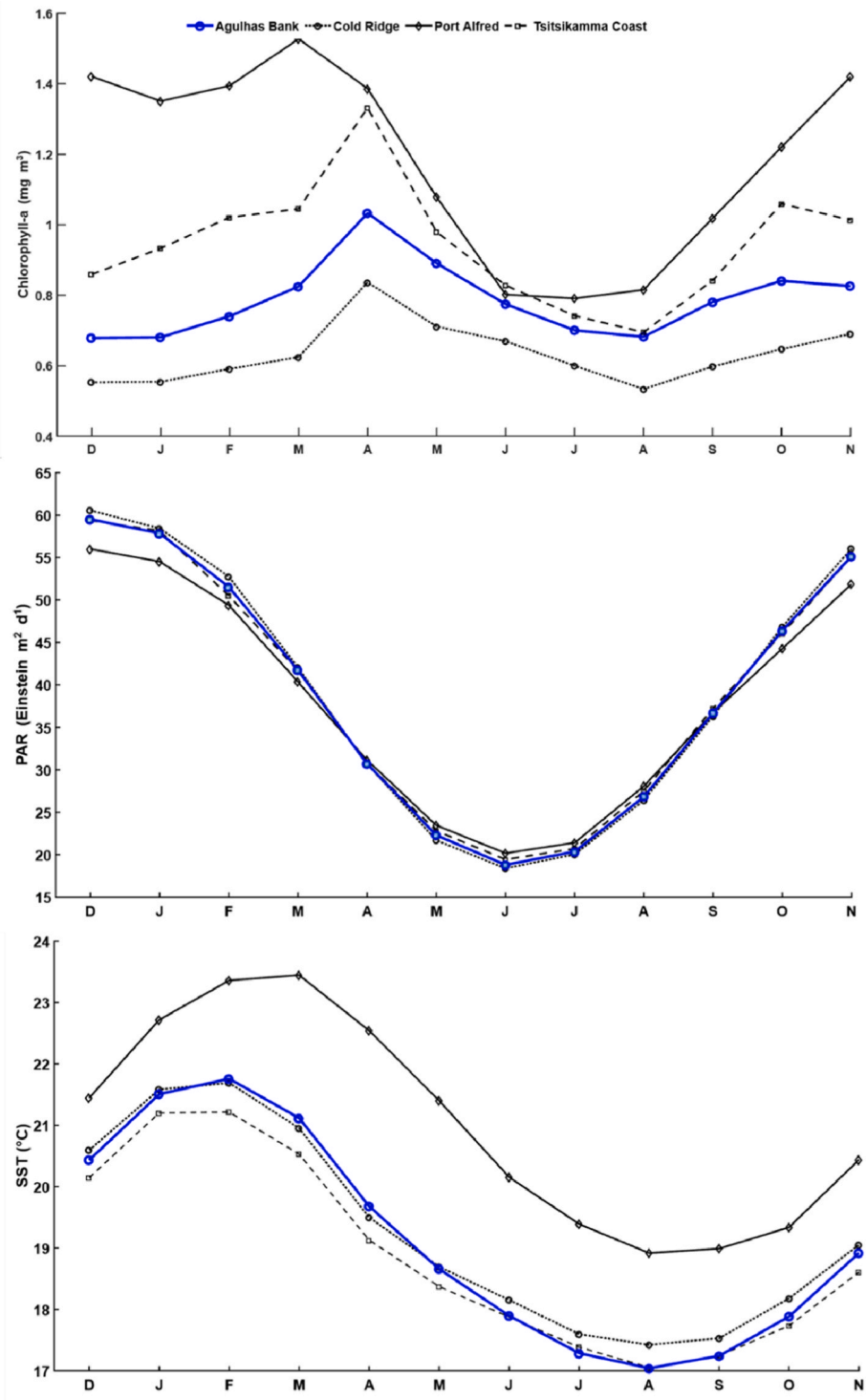

Fig. 7. Monthly climatology for Chlorophyll-a (mg m^{-3}) (a), PAR (Einstein m^{-2} d^{-1}) (b) and SST (°C) (c) for the AB and specific upwelling cells on the Agulhas bank shelf for the years 1998 to 2018.

waters in winter on the AB and specific upwelling zones (Fig. 7c). The Port Alfred area also showed higher SST than the other areas (Fig. 7c), likely linked to the proximity of the warm Agulhas Current (Lutjeharms, 2006a).

The AB oceanography is also known to be strongly influenced by surface winds which show seasonality in their strength and direction (Fig. 8). Over the 21-year period, higher wind speeds were observed in winter (2–4.5 ms^{-1}) on the AB and for all the upwelling zones, compared to summer (1.5–3 ms^{-1}) (Fig. 8a). The main wind direction also shifts between seasons, with winters dominated by north-westerly winds, while summers have stronger south-easterly winds (Fig. 8b and c). This climatology of the winds on the AB (Fig. 8) matches with shorter-term studies (e.g., Malan, 2013) and those which predate the availability of satellite-derived wind data (e.g., Swart and Largier, 1987; Hutchings, 1994).

Seasonal changes in the NPP are caused by changes in phytoplankton biomass and the environmental factors that control their growth, such as light, temperature and nutrient availability, which all influence the

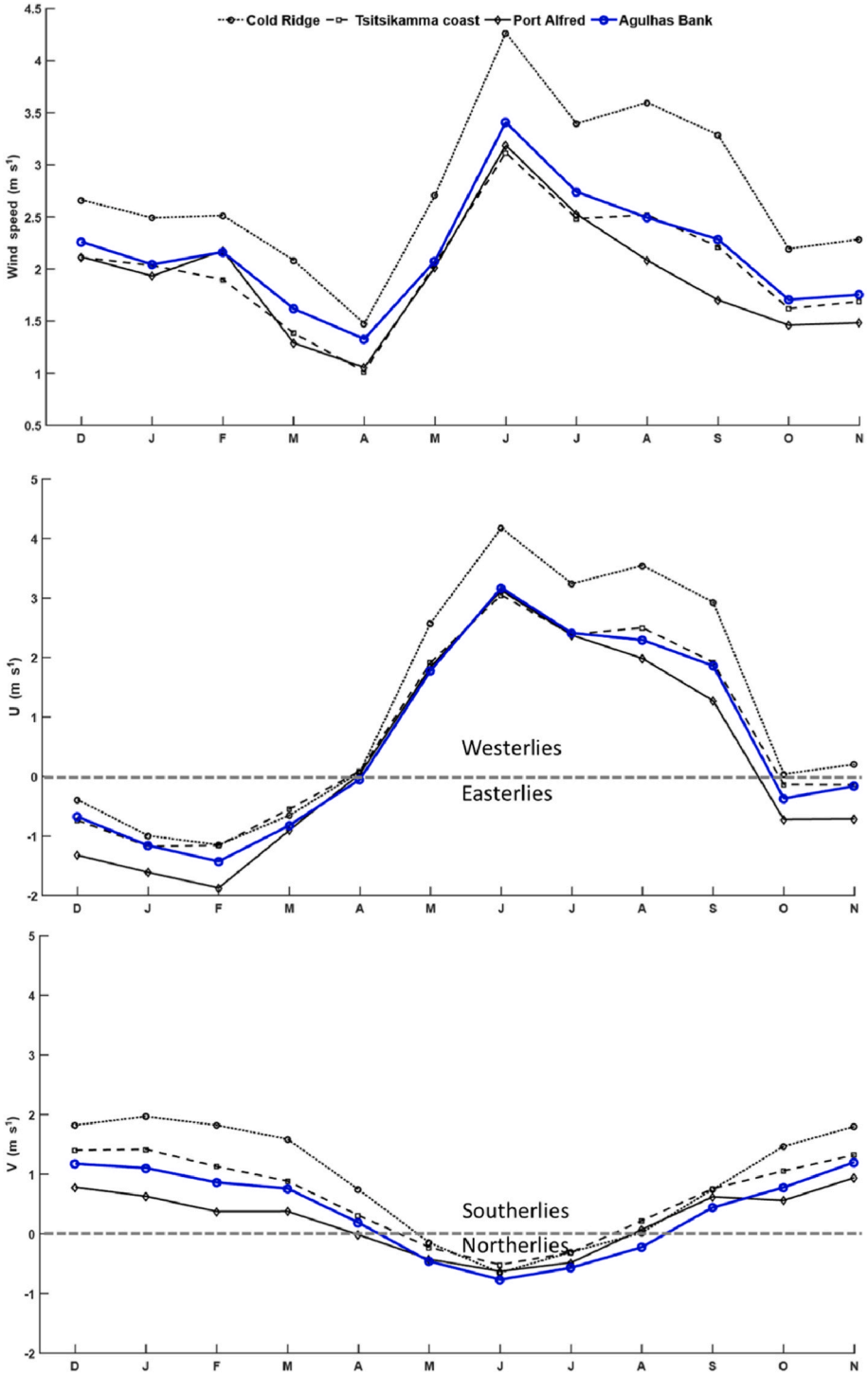

Fig. 8. Climatology of (a) wind speed, (b) E-W component (U) and (c) N–S component (V) for the AB shelf and specific upwelling zones on the AB shelf for the 21-year period (1998 – 2018). The negative values in plot (b) indicate east to west winds and the positive values indicate west to east winds, in plot © the negative values indicate north to south winds and the positive values indicate the south to north winds.

physiology of phytoplankton (e.g., Kong et al., 2019). During dark winter conditions, the strong north-westerly winds (Fig. 8) result in a deepening of the mixed layer (80–90 m) (Swart and Largier, 1987; Hutchings, 1994; Boyd and Shillington, 1994) which induces mixing of the deep nutrient-rich waters into the upper water column. This will allow phytoplankton to grow as soon as the light and temperature levels increase in late winter/early spring. The low chlorophyll-*a* values on the AB during summer have been recorded in this study (Fig. 7a) as well as by Brown (1992), and are attributed to nutrient-limitation caused by a stronger stratification of the water column (De Villiers, 1998). Strong stratification also leads to an increase of biomass at depth (Subsurface Chlorophyll-*a* Maximum), close to the nutricline and at low light levels (Carter et al., 1987; Poulton et al., *this issue*), which is not considered using remote sensing data.

The NPP difference between seasons was relatively low and restricted to ~1 g C m^{-2} d^{-1} (Fig. 3; Table 2). The AB does not seem to experience the strong seasonal changes in NPP seen in other shelf systems, mostly due to the relatively high NPP in winter (~1 g C m^{-2} d^{-1}) compared to many other shelf seas which have much lower NPP in winter (0.2–0.4 g C m^{-2} d^{-1} based on remote sensing estimations) (e.g., Curran et al., 2018; Thompson and Mcdonald, 2020; Joint et al., 2001; Curran et al., 2018; Beca-Carretero et al., 2019; Cervantes-Duarte et al., 2021). On the North-western European Shelf, for instance, NPP only increases above 1 g C m^{-2} d^{-1} for 3 months of the year (May, June and September) (Joint et al., 2001; Curran et al., 2018) while NPP never goes below this value on the AB. Similarly, annual NPP on the Northwest Iberian Margin remains below 1 g C m^{-2} d^{-1} for 7 months (October to April) (Beca-Carretero et al., 2019), while in Bahia De La Paz (Mexico, 24–25 °N), the seasonal NPP remains below 1 g C m^{-2} d^{-1} for 6 months (July to November) (Cervantes-Duarte et al., 2021). The annual average NPP estimation on the AB (516 g C m^{-2} yr^{-1}) is higher in comparison to other shelf seas (see section 4.1). Even if the AB does not have extremely high monthly average NPP values as mentioned above, the semi-constant NPP throughout the seasons explains its overall high annual productivity compared with other shelf systems (e.g., 385 g C m^{-2} yr^{-1}; Longhurst et al., 1995).

A possible explanation for the lack of strong seasonality on the AB, with NPP remaining >1 g C m^{-2} d^{-1} for much of the year, may lie in the oceanographic dynamics of the AB which are driven by a feature unique to the AB – the Agulhas Current. As well as stabilizing and strengthening the AB thermocline through the provision of warm surface water (Jury, 1994; Lutjeharms, 2006a, 2206b), the Agulhas Current also supports the encroachment of nutrient-rich South Indian Central Water into the shelf bottom waters (Lutjeharms, 2006a, 2006b); thus, the Agulhas Current reinforces both the thermal stratification of the shelf waters and the vertical nutrient gradient. To support relatively high productivity throughout the year, as observed by this study, the sunlit surface waters of the AB must be fed by regular inputs of nutrients. Coastal upwelling is well known on the AB (e.g., Roberts and van den Berg, 2005; Goschen and Schumann, 2011; Duncan et al., 2019), supplied by the continuously enriched shelf bottom waters, and thermocline dynamics, be it internal waves or phytoplankton growing at depth in the Subsurface Chlorophyll-*a* Maximum (Poulton et al., *this issue*), will control the supply of nutrients to the upper productive waters. Some *in-situ* observations in the CAB have suggested that while the thermocline deepens in winter, it does not completely disappear (Carter et al., 1987) and the system appears to remain stratified.

With an annual amplitude of variability of chlorophyll-*a* of only 0.3 mg m^{-3} (Fig. 7a) and NPP of only 1 g C m^{-2} d^{-1} (Fig. 3), the AB does not appear to exhibit strong seasonal blooms in spring or autumn, with NPP remaining >1 g C m^{-2} d^{-1} for much of the year. In many shelf systems, these seasonal blooms are a result of wintertime overturning of the water column, resetting nutrient levels to high pre-spring levels (e.g., Poulton et al., 2019). With the continuous reinforcement of the AB thermocline by the Agulhas Current, it seems reasonable to hypothesize that the AB does not experience a wide-spread wintertime breakdown of stratification, resetting nutrients to high levels, but experiences a steady flux of nutrients across the thermocline (potentially regulated by internal dynamics of the thermocline; Poulton et al., *this issue*) that supports a continuous, moderate level of NPP all year around. A severe lack of wintertime measurements of nutrients, water column structure or phytoplankton productivity inhibits further testing of this hypothesis; clearly, understanding the annual cycle of oceanographic dynamics on the AB is thus an important step forward.

Despite only a moderate amplitude of seasonal variability of NPP on the AB, it was stronger along the coast and on the EAB than on the CAB (Fig. 2c). This may be related to the functioning of the EAB. The EAB is relatively narrow and might be more influenced by the shelf break upwelling than the CAB (Lutjeharms, 2006a; Malan, 2013; Krug et al., 2014). This is in agreement with the lack of seasonality of the Agulhas Current in terms of its position relative to the shelf (Krug and Tournadre, 2012). However, some studies have also shown changes in the speed of the Agulhas Current with greater flow in austral spring/summer (Lutjeharms, 2006a; Krug and Tournadre, 2012; Hutchinson et al., 2018), with a possible influence on the amount of shelf-edge upwelling. The coastal areas of the AB are prone to wind-driven upwelling which are triggered by easterly winds dominant in the summer months (Fig. 8; e.g., Boyd and Shillington, 1994; Goschen and Schumann, 2011; Duncan et al., 2019). This has been shown especially for the coastal bays (Goschen et al., 2015) and could explain the seasonality of the NPP we observed in the inshore grounds of Tsitsikamma (Fig. 4). For Port Alfred, however, Malan (2013) showed that wind is not the primary driver of the upwelling and that other mechanisms might be at play (e.g., variability in bottom water encroachment onto the shelf).

4.4. Temporal variability of Net Primary Production on the Agulhas Bank

With 21 years of satellite data available, it is now possible to examine long-term decadal trends in NPP on the AB, in terms of both the magnitude of interannual variability (Fig. 6) and long-term trends (Fig. 6c). In this study we used a blended chlorophyll-*a* product (OC–CCI) which is the most consistent record throughout the time, particularly when considering both periods, before and after 2002 (Couto et al., 2016). The merged product can, however, overestimate chlorophyll-*a* in coastal areas, as noted by Sathyendranath et al. (2020). However, in their study, Couto et al. (2016) found that the OC-CCI is still amongst the "best" and consistent products for chlorophyll-*a*. The OC-CCI product is considered especially reliable given that this is a longer merged dataset than single sensor timeseries and additionally features corrected drift in the MODIS sensor (Jackson et al., 2020). The multi-sensor OC-CCI product also features MERIS which gets closer to the coast than the other ocean colour sensors, and provides overall an improved performance in Case-2 (coastal) waters as well as Case-1 open waters (Jackson et al., 2020). NPP calculated using the MODIS chlorophyll-*a* product was dissimilar to that calculated using OC-CCI chlorophyll-*a*. Therefore, NPP estimation based on satellite may vary slightly, depending on the chlorophyll-*a* product used (single or multi-mission sensors). Years with low annual NPP (Fig. S1) generally have low NPP across the entire AB (Fig. S1), with a slight tendency for higher NPP off Port Alfred. In contrast, during years with high NPP, specific hotspots can be observed in different areas of the bank, mostly (<100 m). For example, the low NPP observed in 2004, 2007 and 2012 was more common over the eastern side of the shelf, whereas when the NPP was high in 2008, 2011 and 2014, there was high NPP over the entire shelf, extending to the cold ridge area (Fig. S1). This indicates that there were most likely more upwelled cold nutrient-enriched waters during these years on the bank, suggesting strong bottom-up (resource) control during these periods.

The long-term annual changes in the NPP on the AB were analysed pixel by pixel (Fig. 6c) and showed a clear decline in the NPP over time on the CAB (20–24°E) between the 100 and 200 m isobath. Demarcq et al. (2008) observed an increase in winds from 1998 to 2007 on the AB,

which can be related to the decline in the NPP over time. Further investigation into the long-term variability of NPP for different seasons showed that these long-term trends do not occur during all seasons (Fig. S2), suggesting that different oceanographic processes are taking place. This implies that the drivers of the long-term trend in NPP differ spatially along the bank, as does the influence, for example, the Agulhas Current and the way it interacts with the bank waters in both the surface and deep layers. In winter, a long-term decrease occurs along most of the shelf break of the AB (Fig. S2) which could be linked to the position and/or intensity of the Agulhas Current. However, as mentioned above, it is not clear whether the Agulhas Current has a clear seasonal trend, or, indeed, if its influence on the AB has a seasonal component, and thus this hypothesis would not explain why these long-term changes are only happening in winter. In the summer months, the area around Port Alfred (26.5–28 °E) showed an increasing trend in the NPP (Fig. S2) in stark contrast to the trend seen elsewhere on the bank. Such an increasing trend might be linked to the easterly winds which are dominant during the summer months (Fig. 7) and can thus trigger coastal wind-driven upwelling. This is in agreement with Lamont et al. (2018) who found an increase in the number of wind-driven upwelling days from 1979 to 2015 on the whole AB, although caution should be taken as the region highlighted here is relatively small and localized.

To fully examine these processes, one would need to investigate anomalies against the different potential drivers (e.g., SST, wind speed, wind direction, wind curl) and the dynamics of the large-scale oceanographic features further afield that directly influence the AB (e.g., Agulhas Current flow and meanders, Agulhas Current temperature anomalies, which could influence the AB thermocline). That several of these drivers are involved in the VGPM algorithm (SST, PAR) further complicates any potential analysis of the long-term trend in NPP.

Many marine ecosystems are considered threatened through declining NPP (e.g., North Sea, Australian region) (Capuzzo et al., 2017; Thompson and Mcdonald, 2020) as a result of climate change, with ocean warming enhancing stratification and reducing nutrient availability. Over the last 21 years, NPP on the AB has only declined by 0.26% per year, a small reduction compared with the declines seen in other marine environments (e.g., 12% in the Australian region; Thompson and Mcdonald, 2020). A reduced decline in the NPP could be due to various mechanisms associated with how nutrients are supplied to the AB, such as the deep advection of South Indian Central Water related to the strength and variability of the Agulhas Current. In this study, the data only covers two decades (21 years) which might also be too short to properly assess long-term climatic trends. The seminal work of Henson et al. (2013) states that "at least 40 years of satellite data is needed to detect anthropogenic signals from natural variability", and hence there is a need to gather more data on the AB to fully examine changes over long-time scales.

4.5. Implications for ecosystem productivity

The findings of this study indicate that the AB is a moderately productive shelf-system, higher in terms of annual NPP than many other shelf-seas, mostly due to its high NPP values in winter (>0.5 g C m^{-2} d^{-1}), though not as productive as upwelling environments. Seasonality on the AB in terms of NPP has a small annual magnitude (~1 g C m^{-2} d^{-1}), with only slightly higher NPP occurring in summer and autumn than during winter. Such small-scale seasonal variability provides an environment that is relatively productive all year round, and hence there is an abundance of primary production to fuel marine ecosystems across the AB throughout the year. The remarkable magnitude and seasonal stability of NPP on the AB likely underpins its importance for supporting regional fish stocks and, in turn, economically important local fisheries. Over the length of the satellite record (1998–2018) examined here, there is also only a minor decline in NPP (0.26% yr^{-1}), with important spatial and temporal variations. Primary production on the AB appears decoupled from large-scale climatic phenomena that are known to influence other marine ecosystems. The importance of the dynamics of the Agulhas Current, one of the largest western Boundary Currents in the world (e.g., transports 70 × 10^6 m^3 s^{-1} of water; Bryden and Beal, 2001; Cásal et al., 2009), for nutrient supply may help to stabilize the NPP dynamics of the AB. However, Asdar et al. (*this issue*) have shown potential future variability in the Agulhas Current which will have important impacts on the AB. These authors found that, while integrated nutrients are projected to decline on the AB, this will not affect NPP significantly, with a fairly stable time-series projected until 2100, especially on the CAB. They also observed an onshore shift of the Agulhas Current which has implications for upwelling on the shelf, affecting the current flow on the AB itself. Future studies need to focus on the dynamics of NPP on the entire shelf – not just on specific regional upwelling sites – as well as the central and eastern regions. There are numerous potential avenues for continuous monitoring of NPP on the AB at both short and long-timescales through the application of satellite-derived NPP.

Author contributions

Sixolile L. Mazwane: Conceptualization, Investigation, Formal analysis, Writing - original draft, Writing - review & editing. **Alex J. Poulton:** Supervision, Conceptualization, Investigation, Formal analysis, Writing - original draft, Writing - review & editing. **Anna Hickman:** Data curation, software, Writing - review & editing. **Margaux Noyon:** Supervision, Resources, Formal analysis, Writing - original draft, Writing - review & editing. **Fatma Jebri:** Data curation, Writing - review & editing. **Zoe Jacobs:** Data curation, Writing - review & editing. **Mike Roberts:** Project administration, Funding acquisition.

Author statement

The authors declare that they have no known competing financial interests or personal relationships that could have appeared to influence the work reported in this paper.

Declaration of competing interest

The authors declare that they have no known competing financial interests or personal relationships that could have appeared to influence the work reported in this paper.

Acknowledgments

This publication was produced with the financial support of the Global Challenges Research Fund (GCRF), UK, in the framework of the SOLSTICE-WIO project, under NERC grant NE/P021050/1. We thank the South African Institute for Aquatic Biodiversity (SAIAB) – ACEP Ph. D. Bursary and the Nelson Mandela University Postgraduate Scholarship for funding and support. This work is also part of the UK-SA bilateral chair Ocean Science and marine food security funded by the NRF/DST Grant (98399) and the British Council grant SARCI150326116102. We would like to thank the Copernicus Marine Environment Service (CMEMS) for providing the SST data (https://www.marine.copernicus.eu) and the ESA Ocean Colour CCI project for processing and providing the *Chl-a* and K_d490 dataset online at http://www.esa-oceancolour-cci.org/. We would also like to thank GlobColour for processing and providing the PAR data (http://hermes.acri.fr/index.php?class=archive). We thank Dionysios Raitsos, Francesco Nencioli, and Giuseppe Foti for helping with the coding on MATLAB.

Appendix A. Supplementary data

Supplementary data to this article can be found online at https://doi.org/10.1016/j.dsr2.2022.105079.

References

Asdar, S., Jacobs, Z., Popova, E., Roberts, M. J., This issue. Impact of climate change on the Agulhas Bank, South Africa – a 80-year projection with consequences for the squid fishery. Deep-Sea Res.

Balkanski, Y., Monfray, P., Battle, M., Heimann, M., 1999. Ocean primary production derived from satellite data: an evaluation with atmospheric oxygen measurements. Global Biogeochem. Cycles 13, 257–271.

Barlow, R., Lamont, T., Kyewalyanga, M., Sessions, H., Morris, T., 2010. Phytoplankton production and physiological adaptation on the southeastern shelf of the Agulhas ecosystem. Continent. Shelf Res. 30, 1472–1486. https://doi.org/10.1016/j.csr.2010.05.007.

Barlow, R., Lamont, T., Mitchell-Innes, B., Lucas, M., Thomalla, S., 2009. Primary production in the Benguela ecosystem. Afr. J. Mar. Sci. 31, 97–101. https://doi.org/10.2989/AJMS.2009.31.1.9.780.

Barnes, B.B., Hu, C., Schaeffer, B.A., Lee, Z., Palandro, D.A., Lehrter, J.C., 2013. MODIS-derived spatiotemporal water clarity patterns in optically shallow Florida Keys waters: a new approach to remove bottom contamination. Remote Sens. Environ. 134, 377–391. https://doi.org/10.1016/j.rse.2013.03.016.

Bauer, J.E., Cai, W.J., Raymond, P.A., Bianchi, T.S., Hopkinson, C.S., Regnier, P.A.G., 2013. The changing carbon cycle of the coastal ocean. Nature 504, 61–70. https://doi.org/10.1038/nature12857.

Beardall, J., Berman, T., Heraud, P., Kadiri, M.O., Light, B.R., Patterson, G., Roberts, S., Sulzberger, B., Sahan, E., Uehlinger, U., Wood, B., 2001. A Comparison of Methods for Detection of Phosphate Limitation in Microalgae, 63, pp. 107–121.

Beca-Carretero, P.P., Otero, J., Land, P.E., Groom, S., Álvarez-Salgado, X.A., 2019. Seasonal and inter-annual variability of net primary production in the NW Iberian margin (1998–2016) in relation to wind stress and sea surface temperature. Prog. Oceanogr. 178, 102135 https://doi.org/10.1016/j.pocean.2019.102135.

Behrenfeld, M.J., Falkowski, P.G., 1997. Photosynthetic rates derived from satellite-based chlorophyll concentration. Limnol. Oceanogr. 42, 1–20. https://doi.org/10.4319/lo.1997.42.1.0001.

Behrenfeld, M.J., Boss, E.D., Siegel, A., Shea, D.M., 2005. Carbon-based ocean productivity and phytoplankton physiology from space. Global Biogeochem. Cycles 19, GB1006. https://doi.org/10.1029/2004GB002299.

Behrenfeld, M.J., O'Malley, R.T., Siegel, D.A., McClain, C.R., Sarmiento, J.L., Feldman, G.C., Milligan, A.J., Falkowski, P.G., Letelier, R.M., Boss, E.S., 2006. Climate-driven trends in contemporary ocean productivity. Nature 444, 752–755. https://doi.org/10.1038/nature05317.

Behrenfeld, M.J., Randerson, J.T., Mcclain, C.R., Gene, C., Los, S.O., Tucker, C.J., Falkowski, P.G., Field, C.B., Frouin, R., Esaias, W.E., Kolber, D.D., Pollack, N.H., Mcclain, R., Gene, G.C., Falkowski, P.G., Field, C.B., Field, C.B., 2001. Primary production production during during an ENSO. Science 291 (80), 2594–2597.

Boyd, A.J., Shillington, F.A., 1994. Physical forcing and circulation patterns on the. Agulhas Bank 90, 114–122.

Boyd, A.J., Taunton-Clark, J., Oberholster, G.P.J., 1992. Spatial features of the near-surface and midwater circulation patterns off western and southern South Africa and their role in the life histories of various commercially fished species. S. Afr. J. Mar. Sci. 12, 189–206. https://doi.org/10.2989/02577619209504702.

Boyd, P.W., Sundby, S., Pörtner, H.-O., 2014. Cross-chapter box on net primary production in the ocean. In: Field, C.B., Barros, V.R., Dokken, D.J., Mach, K.J., Mastrandrea, M.D., Bilir, T.E., Chatterjee, M., Ebi, K.L., Estrada, Y.O., Genova, R.C., Girma, B., Kissel, E.S., Levy, A.N., MacCracken, S., Mastrandrea, P.R., White, L.L. (Eds.), Climate Change 2014: Impacts, Adaptation, and Vulnerability. Part A: Global and Sectoral Aspects. Contribution of Working Group II to the Fifth Assessment Report of the Intergovernmental Panel on Climate Change. Cambridge University Press, United Kingdom and New York, pp. 133–136.

Brown, P.C., 1984. Primary production at two contrasting nearshore sites in the Southern Benguela upwelling region, 1977—1979. S. Afr. J. Mar. Sci. 2, 205–215. https://doi.org/10.2989/02577618409504369.

Brown, P.C., 1992. Spatial and seasonal variation in chlorophyll distribution in the upper 30 m of the photic zone in the southern Benguela/Agulhas ecosystem. S. Afr. J. Mar. Sci. 12 (1), 515–525. https://doi.org/10.2989/02577619209504722.

Bryden, H.L., Beal, L.M., 2001. Role of the Agulhas Current in Indian Ocean circulation and associated heat and freshwater fluxes. Deep. Res. Part I Oceanogr. Res. Pap. 48, 1821–1845. https://doi.org/10.1016/S0967-0637(00)00111-4.

Campbell, J., Antoine, D., Armstrong, R., Arrigo, K., Balch, W., Barber, R., Behrenfeld, M., Bidigare, R., Bishop, J., Carr, M., Esaias, W., Falkowski, P., Hoepffner, N., Iverson, R., Kiefer, D., Lohrenz, S., Marra, J., 2002. Comparison of Algorithms for Estimating Ocean Primary Production from Surface Chlorophyll, Temperature, and Irradiance 16.

Capuzzo, E., Lynam, C.P., Barry, J., Stephens, D., Forster, R.M., Greenwood, N., McQuatters-Gollop, A., Silva, T., van Leeuwen, S.M., Engelhard, G.H., 2017. A decline in primary production in the North Sea over 25 years, associated with reductions in zooplankton abundance and fish stock recruitment. Global Change Biol. 24, e352–e364. https://doi.org/10.1111/gcb.13916.

Carter, R.A., McMurray, H.F., Largier, J.L., 1987. Thermocline characteristics and phytoplankton dynamics in Agulhas bank waters. S. Afr. J. Mar. Sci. 5, 327–336. https://doi.org/10.2989/025776187784522306.

Cásal, T.G.D., Beal, L.M., Lumpkin, R., Johns, W.E., 2009. Structure and downstream evolution of the Agulhas Current system during a quasi-synoptic survey in February-March 2003. J. Geophys. Res. Ocean. 114, 1–16. https://doi.org/10.1029/2008JC004954.

Cervantes-Duarte, R., González-Rodríguez, E., Funes-Rodríguez, R., Ramos-Rodríguez, A., Torres-Hernández, M.Y., Aguirre-Bahena, F., 2021. Variability of net primary productivity and associated biophysical drivers in bahía de La Paz (Mexico). Rem. Sens. 13 (9), 1644. https://doi.org/10.3390/rs13091644.

Chang, N., 2008. Numerical Ocean Model Study of the Agulhas Bank and the Cool Ridge. Univ., Cape T.

Chapman, P., Largier, J., 1989. On the origin of Agulhas Bank water. South Afr. J. Sci. 85, 515–519.

Couto, A.B., Brotas, V., Mélin, F., Groom, S., Sathyendranath, S., 2016. Inter-comparison of OC-CCI chlorophyll-*a* estimates with precursor data sets. Int. J. Rem. Sens. 37 (18), 4337–4355. https://doi.org/10.1080/01431161.2016.1209313.

Curran, K., Brewin, R.J.W., Tilstone, G.H., Bouman, H.A., Hickman, A., 2018. Estimation of size-fractionated primary production from satellite ocean colour in UK shelf seas. Rem. Sens. 10, 1389. https://doi:10.3390/rs10091389.

De Villiers, S., 1998. Seasonal and interannual variability in phytoplankton biomass on the southern African continental shelf: evidence from satellite-derived pigment concentrations. S. Afr. J. Mar. Sci. 19, 169–179. https://doi.org/10.2989/025776198784126872.

Demarcq, H., Richardson, A.J., Field, J.G., 2008. Generalised model of primary production in the southern Benguela upwelling system. Mar. Ecol. Prog. Ser. 354, 59–74. https://doi.org/10.3354/meps07136.

Deng, Y., Zhang, Yunlin, Li, D., Shi, K., Zhang, Yibo, 2017. Temporal and spatial dynamics of Phytoplankton primary production in Lake Taihu derived from MODIS data. Rem. Sens. 9 https://doi.org/10.3390/rs9030195.

Duncan, M.I., James, N.C., Bates, A.E., Goschen, W.S., Potts, W.M., 2019. Localised intermittent upwelling intensity has increased along South Africa's south coast due to El Niño–Southern Oscillation phase state. Afr. J. Mar. Sci. 41, 325–330. https://doi.org/10.2989/1814232X.2019.1656105.

Eppley, R., Steward, E., Abbott, M., Heyman, U., 1985. Estimating Ocean primary production from satellite chlorophyll: introduction to regional differences and statistics for the southern California Bight. J. Plankton Res. 7, 57–70. https://doi.org/10.1093/plankt/7.1.57.

Gill, A.E., Schumann, E.H., 1979. Topography induced changes in the structure of an inertial coastal jet: application to the Agulhas current. Am. Meteorol. Soc. 9, 975–990.

Gordon, A.L., 2003. The brawniest retroflection. Nature 421, 904–905. https://doi.org/10.1038/421904a.

Goschen, W.S., Bornman, T.G., Deyzel, S.H.P., Schumann, E.H., 2015. Coastal upwelling on the far eastern Agulhas Bank associated with large meanders in the Agulhas Current. Continent. Shelf Res. 101, 34–46. https://doi.org/10.1016/j.csr.2015.04.004.

Goschen, W.S., Schumann, E.H., 2011. The Physical Oceanographic Processes of Algoa Bay, with Emphasis on the Western Coastal Region: A Synopsis of the Main Results of Physical Oceanographic Research Undertaken in and Around Algoa Bay up until 2010.

Goschen, W.S., Schumann, E.H., Bernard, K.S., Bailey, S.E., Deyzel, S.H.P., 2012. Upwelling and ocean structures off Algoa Bay and the south-east coast of South Africa. Afr. J. Mar. Sci. 34 (4), 525–536. https://doi.org/10.2989/1814232X.2012.749810.

Goschen, W.S., Schumann, E.H., 1994. An Agulhas current intrusion into Algoa bay during August 1988. S. Afr. J. Mar. Sci. 14, 47–57. https://doi.org/10.2989/025776194784286914.

Grange, S.K., 2014. Technical Note: Averaging Wind Speeds and Directions. Technical Report, University of Auckland, Auckland, New Zealand. https://doi.org/10.13140/RG.2.1.3349.2006, 2014.

Gregg, W.W., Ginoux, P., Schopf, P.S., Casey, N.W., 2003. Phytoplankton and Iron: Validation of a Global Three-Dimensional Ocean Biogeochemical Model, 50, pp. 3143–3169. https://doi.org/10.1016/j.dsr2.2003.07.013.

Henson, S., Cole, H., Beaulieu, C., Yool, A., 2013. The impact of global warming on seasonality of ocean primary Production. Biogeosciences 10, 4357–4369. https://doi.org/10.5194/bg-10-4357-2013, 2013.

Hersbach, H., Bell, B., Berrisford, P., Hirahara, S., Horányi, A., Muñoz-Sabater, J., Nicolas, J., Peubey, C., Radu, R., Schepers, D., Simmons, A., Soci, C., Abdalla, S., Abellan, X., Balsamo, G., Bechtold, P., Biavati, G., Bidlot, J., Bonavita, M., De Chiara, G., Dahlgren, P., Dee, D., Diamantakis, M., Dragani, R., Flemming, J., Forbes, R., Fuentes, M., Geer, A., Haimberger, L., Healy, S., Hogan, R.J., Hólm, E., Janisková, M., Keeley, S., Laloyaux, P., Lopez, P., Lupu, C., Radnoti, G., de Rosnay, P., Rozum, I., Vamborg, F., Villaume, S., Thépaut, J., 2020. The ERA5 global reanalysis. Q. J. R. Meteorol. Soc. 146, 1999–2049.

Hooker, S.B., Patt, F.S., Barnes, R.A., Eplee, R.E., Franz, B.A., Robinson, W.D., Feldman, G.C., Bailey, S.W., Gales, J., Werdell, P.J., Wang, M., Frouin, R., Yoder, J. A., 2003. SeaWiFS Postlaunch Technical Report Series Volume 22, Algorithm Updates for the Fourth SeaWiFS Data Reprocessing. Nasa Technical Memorandum.

Hutchings, L., 1994. The Aguhas Bank: a synthesis of available information and a brief comparison with other east-coast shelf regions. South Afr. J. Sci. 90, 179–185.

Hutchings, L., Beckley, L.E., Griffiths, M.H., Roberts, M.J., Sundby, S., Van der Lingen, C., 2002. Spawning on the edge: spawning grounds and nursery areas around the southern African coastline. Mar. Freshw. Res. 53, 307–318.

Hutchinson, K., Beal, L.M., Penven, P., Ansorge, I., Hermes, J., 2018. Seasonal phasing of Agulhas current transport tied to a baroclinic adjustment of near-field winds. J. Geophys. Res. Ocean. 123, 7067–7083. https://doi.org/10.1029/2018JC014319.

IOCCG, 2000. IOCCG Report Number 03: Remote Sensing of Ocean Colour in Coastal, and Other Optically Complex, Waters. IOCCG. Canada.

Jackson, J.M., Rainville, L., Roberts, M.J., McQuaid, C.D., Lutjeharms, J.R.E., 2012. Mesoscale bio-physical interactions between the Agulhas current and the Agulhas bank, South Africa. Continent. Shelf Res. 49, 10–24. https://doi.org/10.1016/j.csr.2012.09.005.

Jackson, T., Chuprin, A., Sathyendranath, S., Grant, M., Zühlke, M., Dingle, J., Storm, T., Boettcher, M., Fomferra, N., 2020. Product User Guide, Ocean Colour Climate Change Initiative (OC_CCI) –Interim Phase. https://docs.pml.space/share/s/dPL4zFuaT_eFa-mTLU9nQA.

Jacobs, Z., Roberts, M., Jebri, J., Srokosz, M., Kelly, S., Sauer, W.H.H., Bruggeman, J., Popova, E. This issue. Drivers of productivity on the Agulhas Bank and the importance for marine ecosystems. Deep-Sea Res. II.

Joint, I., Wollast, R., Chou, L., Batten, S., Elskens, M., Edwards, E., Hirst, A., Burkill, P., Groom, S., Gibb, S., Miller, A., Hydes, D., Dehairs, F., Antia, A., Barlow, R., Rees, A., Pomroy, A., Brockmann, U., Cummings, D., Lampitt, R., Loijens, M., Mantoura, F., Miller, P., Raabe, T., Alvarez-Salgado, X., Stelfox, C., Woolfenden, J., 2001. Pelagic production at the Celtic Sea shelf break. Deep. Res. Part II Top. Stud. Oceanogr. 48, 3049–3081. https://doi.org/10.1016/S0967-0645(01)00032-7.

Jury, M.R., 1994. A review of the meteorology of the eastern Agulhas Bank. South Afr. J. Sci. 90, 109–113.

Kahru, M., Kudela, R., Manzano-Sarabia, M., Mitchell, B.G., 2009. Trends in primary production in the California Current detected with satellite data. J. Geophys. Res. 114, C02004. https://doi.org/10.1029/2008JC004979.

Kameda, T., Ishizaka, J., 2005. Size-fractionated primary production estimated by a two-phytoplankton community model applicable to ocean color remote sensing. J. Oceanogr. 61, 663–672.

Kong, F., Dong, Q., Xiang, K., Yin, Z., Li, Y., Liu, J., 2019. Spatiotemporal variability of remote sensing ocean net primary production and major forcing factors in the tropical eastern Indian and Western Pacific Ocean. Rem. Sens. 11, 1–18. https://doi.org/10.3390/rs11040391.

Krug, M., Tournadre, J., 2012. Satellite observations of an annual cycle in the Agulhas Current. Geophys. Res. Lett. 39 https://doi.org/10.1029/2012GL052335.

Krug, M., Tournadre, J., Dufois, F., 2014. Interactions between the Agulhas current and the eastern margin of the Agulhas bank. Continent. Shelf Res. 81, 67–79. https://doi.org/10.1016/j.csr.2014.02.020.

Kulk, G., Platt, T., Dingle, J., Jackson, T., Jönsson, B.F., Bouman, H.A., Babin, M., Brewin, R.J.W., Doblin, M., Estrada, M., Figueiras, F.G., Furuya, K., González-Benítez, N., Gudfinnsson, H.G., Gudmundsson, K., Huang, B., Isada, T., Kovač, Ž., Lutz, V.A., Marañón, E., Raman, M., Richardson, K., Rozema, P.D., van de Poll, W.H., Segura, V., Tilstone, G.H., Uitz, J., van Dongen-Vogels, V., Yoshikawa, T., Sathyendranath, S., 2021. Primary production, an index of climate change in the ocean: satellite-based estimates over two decades. Rem. Sens. 13 (17), 3462. https://doi.org/10.3390/rs13173462.

Lamont, T., 2011. Bio-optical Investigation of Phytoplankton Production in the Southern Benguela Ecosysytem. University of Cape, Town, South Africa, p. 129. PhD Thesis.

Lee, Z., Marra, J., Perry, M.J., Kahru, M., 2015. Estimating oceanic primary productivity from ocean color remote sensing: a strategic assessment. J. Mar. Syst. 149, 50–59. https://doi.org/10.1016/j.jmarsys.2014.11.015.

Lamont, T., García-Reyes, M., Bograd, S.J., van der Lingen, C.D., Sydeman, W.J., 2018. Upwelling indices for comparative ecosystem studies: Variability in the Benguela Upwelling System. J. Mar. Syst. 188, 3–16. https://doi.org/10.1016/j.jmarsys.2017.05.007.

Lee, Z.P., Du, K.P., Arnone, R., 2005. A model for the diffuse attenuation coefficient of downwelling irradiance. J. Geophys. Res. C Oceans 110, 1–10. https://doi.org/10.1029/2004JC002275.

Li, W., Tiwari, S.P., El-Askary, H.M., Qurban, M.A., Amiridis, V., ManiKandan, K.P., Garay, M.J., Kalashnikova, O.V., Piechota, T.C., Struppa, D.C., 2020. In: Synergistic Use of Remote Sensing and Modeling for Estimating Net Primary Productivity in the Re, 12, pp. 8717–8734.

Lohrenz, S.E., Redalje, D.G., Verity, P.G., Flagg, C.N., Matulewski, K.V., 2002. Primary Production on the Continental Shelf off Cape Hatteras, North Carolina, Deep-Sea Research Part II: Topical Studies in Oceanography. https://doi.org/10.1016/S0967-0645(02)00126-1.

Lomas, M.W., Moran, S.B., Casey, J.R., Bell, M., Tiahlo, D.W., Whitefield, J., Kelly, R.P., Mathis, J.T., Cokelet, E.D., 2012. Spatial and seasonal variability of primary production on the Eastern Bering Sea shelf. Deep-Sea Res. II. 65–70, 126–140. https://doi:10.1016/j.dsr2.2012.02.010.

Longhurst, A., Sathyendranath, S., Platt, T., Caverhill, C., 1995. An estimate of global primary production in the ocean from satellite radiometer data. J. Plankton Res. 17, 1245–1271. https://doi.org/10.1093/plankt/17.6.1245.

Lutjeharms, J.R.E., Meyer, A.A., Ansorge, I.J., Eagle, G.A., Orren, M.J., 1996. The nutrient characteristics of the Agulhas Bank. S. Afr. J. Mar. Sci. 17 (1), 253–274. https://doi: 10.2989/025776196784158464.

Lutjeharms, J.R.E., 2006a. The Agulhas Current. springer Berlin Heidelberg. https://doi.org/10.1007/3-540-37212-1.

Lutjeharms, J.R.E., 2006b. the Ocean environment off southeastern Africa: a review. South Afr. J. Sci. 102, 41–426. https://doi.org/10.1007/3-540-37212-1.

Ma, S., Tao, Z., Yang, X., Yu, Y., Zhou, X., Ma, W., Li, Z., 2014. Estimation of marine primary productivity from satellite-derived phytoplankton absorption data. IEEE J. Selected Top. Appl. Obs. Remote Sens. 7, 3084–3092.

Malan, N., 2013. Driving Mechanisms of the Port Alfred Upwelling Cell Inshore of the Agulhas Current. MSc Thesis, University of Cape, Town.

Marra, J., Ho, C., Trees, C.C., 2003. An Alternative Algorithm for the Calculation of Primary Productivity from Remote Sensing Data. LDEO Technical Report. Lamont-Doherty Earth Observatory of Columbia University and *Center for Hydrologic Optics and Remote Sensing, San, pp. 1–28.

McMurray, H.F., 1989. Phytoplankton Production in Agulhas Bank Waters (South Africa).

McQuatters-gollop, A., Reid, P.C., Edwards, M., Burkill, P.H., Castellani, C., 2011. http://www.nature.com/nature/journal/v472/n7342/full/nature09950.html. https://doi.org/10.1038/nature09950.

Mizobata, K., Saitoh, S., 2004. Variability of Bering Sea eddies and primary productivity along the shelf edge during 1998–2000 using satellite multisensor remote sensing. J. Mar. Syst. 50, 101–111. https://doi:10.1016/j.jmarsys.2003.09.014.

Morel, A., Gentili, B., Chami, M., Ras, J., 2006. Bio-optical properties of high chlorophyll Case 1 waters and of yellow- substance-dominated Case 2 waters. Deep-Sea Res. 53, 1439–1459.

Muller-Karger, F.E., Varela, R., Thunell, R., Luerssen, R., Hu, C., Walsh, J.J., 2005. The importance of continental margins in the global carbon cycle. Geophys. Res. Lett. 32, 1–4. https://doi.org/10.1029/2004GL021346.

Pauly, D., Christensen, V., Guénette, S., Pitcher, T.J., Sumaila, U.R., Walters, C.J., Watson, R., Zeller, D., 2002. Towards sustainability in world fisheries. Nature 418, 689–695. https://doi.org/10.1038/nature01017.

Poulton, A.J., Stinchcombe, M.C., Achterberg, E.P., Bakker, D.C.E., Dumousseaud, C., Lawson, H.E., Lee, G.A., Richier, S., Suggett, D.J., Young, J.R., 2014. Coccolithophores on the north-west European shelf: calcification rates and environmental controls. Biogeosciences 11, 3919–3940. https://doi.org/10.5194/bg-11-3919-2014.

Poulton, A.J., Davis, C.E., Daniels, C.J., Mayers, K.M.J., Harris, C., Tarran, G.A., Widdicombe, C.E., Woodward, E.M.S., 2019. Seasonal phosphorus and carbon dynamics in a temperate shelf sea (Celtic Sea). Prog. Oceanogr. 177, 101872 https://doi.org/10.1016/j.pocean.2017.11.001.

Poulton, A.J., Mazwane, S.L., Godfrey, B., Carvalho, A., Mawji, E., Wihsgott, J.U., Noyon, M., This issue. Primary production dynamics on the Agulhas Bank in autumn. Deep-Sea Res.. II.

Probyn, T.A., Mitchell-Innes, B.A., Searson, S., 1995. Primary productivity and nitrogen uptake in the subsurface chlorophyll-*a* maximum on the Eastern Agulhas Bank. Continent. Shelf Res. 15, 1903–1920. https://doi.org/10.1016/0278-4343(94)00099-9.

Probyn, T.A., Mitchellinnes, B.A., Brown, P.C., Hutchings, L., Carter, R.A., 1994. A Review of primary production and related processes on the Agulhas Bank. South Afr. J. Sci. 90, 166–173.

Racault, M.F., Sathyendranath, S., Brewin, R.J.W., Raitsos, D.E., Jackson, T., Platt, T., 2017. Impact of El Niño variability on oceanic phytoplankton. Front. Mar. Sci. 4, 133. https://doi.org/10.3389/fmars.2017.00133.

Roberts, M.J., 2005. Chokka squid (Loligo vulgaris reynaudii) abundance linked to changes in South Africa's Agulhas Bank ecosystem during spawning and the early life cycle. ICES (Int. Counc. Explor. Sea) J. Mar. Sci. 62 (1), 33–55. https://doi.org/10.1016/j.icesjms.2004.10.002.

Roberts, M.J., van den Berg, M., 2005. Currents along the Tsitsikamma coast, South Africa, and potential transport of squid paralarvae and ichthyoplankton. Afr. J. Mar. Sci. 27 (2), 375–388. https://doi.org/10.2989/18142320509504096.

Roberts, M. J., This issue. The South African squid fishery – why do catches crash intermittently? Deep-Sea Res. II.

Sathyendranath, S., Jackson, T., Brockmann, C., Brotas, V., Calton, B., Chuprin, A., Clements, O., Cipollini, P., Danne, O., Dingle, J., Donlon, C., Grant, M., Groom, S., Krasemann, H., Lavender, S., Mazeran, C., Mélin, F., Moore, T.S., Müller, D., Regner, P., Steinmetz, F., Steele, C., Swinton, J., Valente, A., Zühlke, M., Feldman, G., Franz, B., Frouin, R., Werdell, J., Platt, T., 2020. ESA Ocean Colour Climate Change Initiative (Ocean_Colour_cci): Version 4.2 Data. Centre for Environmental Data Analysis. https://doi.org/10.5285/d62f7f801cb54c749d20e736d4a1039f, 19 May 2021.

Schumann, E.H., 1987. The coastal ocean off the east coast of South Africa. Trans. Roy. Soc. S. Afr. 46 (3), 215–229.

Simpson, J.H., Sharples, J., 2012. Introduction to the Physical and Biological Oceanography of Shelf Seas. Cambridge University Press. https://doi.org/10.1017/CBO9781107415324.004.

Smyth, T.J., Pemberton, K.L., Aiken, J., Geider, R.J., 2004. A methodology to determine primary production and phytoplankton photosynthetic parameters from Fast Repetition Rate Fluorometry. J. Plankton Res. 26, 1337–1350. https://doi.org/10.1093/plankt/fbh124.

South African Weather Services (SAWS), 2020. Climate and Water, Annual Report 2019/20. South Africa, Pretoria.

Swart, V.P., Largier, J.L., 1987. Thermal structure of Agulhas bank water. S. Afr. J. Mar. Sci. 5, 243–252. https://doi.org/10.2989/025776187784522153.

Taboada, F.G., Bartona, A.D., Stockb, C.A., Dunne, J., John, J.G., 2019. Seasonal to interannual predictability of oceanic net primary production inferred from satellite observations. Prog. Oceanogr. 170, 28–39. https://doi.org/10.1016/j.pocean.2018.10.010.

Testa, G., Masotti, I., Farías, L., 2018. Temporal variability in net primary production in an upwelling area off Central Chile (36∘S). Front. Mar. Sci. 5, 179. https://doi: 10.3389/fmars.2018.00179.

Thomas, H., Bozec, Y., Elkalay, K., De Baar, H.J.W., 2004. Response to comment on "Enhanced open ocean storage of CO2 from shelf sea pumping. Science 306 (80), 1477d. https://doi.org/10.1126/science.1103193, 1477d.

Thompson, P., Mcdonald, K., 2020. Spatial and Seasonal Trends in Net Primary Production. https://doi.org/10.26198/5e16a4a749e7a.

Verdugo-Díaz, G., Martínez-López, A., Villegas-Aguilera, M.M., Gaxiola-Castro, G., 2014. Primary production and photosynthetic efficiency in Alfonso Basin, La Paz Bay, Gulf of California, Mexico. Rev. Biol. Mar. Oceanogr. 49, 527–536.

Walker, N.D., 1986. Satellite observations of the Agulhas Current and episodic upwelling south of Africa. Deep. Res. 33, 1083–1106.

Watson, R., Pauly, D., 2001. Systematic distortions in world fisheries catch trends. Nature 414, 534–536. https://doi.org/10.1038/35107050.

Yamada, K., Ishizaka, J., Nagata, H., 2005. Spatial and temporal variability of satellite primary production in the Japan sea from 1998 to 2002. J. Oceanogr. 61, 857–869.
Zhang, C., Hu, C., Shang, S., Müller-Karger, F.E., Li, Y., Dai, M., Huang, B., Ning, X., Hong, H., 2006. Bridging between SeaWiFS and MODIS for continuity of chlorophyll-*a* concentration assessments off Southeastern China. Remote Sens. Environ. 102, 250–263.
Zhang, X., Hu, L., 2009. Estimating scattering of pure water from density fluctuation of the refractive index. Opt. Soc. Am. 17, 1671–1678. https://doi.org/10.1364/oe.17.001671.